Separation Science and Technology
Publication details, including instructions for authors and subscription information:
http://www.informaworld.com/smpp/title~content=t713708471

A Variable Molecular Separator

Daryl E. Sharp[a]
[a] ENVIRONMENTAL SCIENCE AND ENGINEERING DEPARTMENT, UNIVERSITY OF NORTH CAROLINA AT CHAPEL HILL, CHAPEL HILL, NORTH CAROLINA

To cite this Article Sharp, Daryl E.(1991) 'A Variable Molecular Separator', Separation Science and Technology, 26: 4, 451 — 502
To link to this Article: DOI: 10.1080/01496399108050485
URL: http://dx.doi.org/10.1080/01496399108050485

SEPARATION SCIENCE AND TECHNOLOGY, **26**(4), pp. 451–502, 1991

A Variable Molecular Separator

DARYL E. SHARP*

ENVIRONMENTAL SCIENCE AND ENGINEERING DEPARTMENT
UNIVERSITY OF NORTH CAROLINA AT CHAPEL HILL
CHAPEL HILL, NORTH CAROLINA 27514

Abstract

The molecular enrichment and carrier gas stream splitting characteristics of a device which functions as a gas chromatograph/mass spectrometer interface are predicted using flow models based on Knudsen's relationships for flow in the transition region between viscous and free molecular flow. These results are compared to experimental measurements of these properties using GC/MS analysis and capacitance manometer pressure measurements. It is suggested that under certain conditions the Knudsen relationships may not apply and that the interface, in conjunction with GC/MS analysis, may be used as a very sensitive probe to investigate the properties of transition gas flow on an accurate quantitative basis. A transition gas flow model is proposed to explain the experimental data in a qualitative sense.

INTRODUCTION

In spite of the success of the technique of inserting the fused silica gas chromatography (GC) column directly into the mass spectrometer (MS) source, the problem of matching the optimum GC flow rate with the flow capacity of the MS remains for most GC/MS analysis. The problem is essentially one of source design rather than pumping speed since the source conductance is usually the limiting factor in determining the source pressure and increases in MS flow capacity by increasing source conductance are generally accomplished at the expense of sensitivity. For low cost instruments without differential pumping, the high vacuum requirement for the mass analyzer section may become a critical factor as well. In these instruments the flow capacity of the MS is usually less than 1 mL/min of helium while the optimum flow rate for the GC column is usually 1.5 mL or more per minute [1.7 sccm (standard cubic centimeters per minute) for a 30-m column with a 0.025-cm i.d.].

*Present address: 2200 Albemarle, #3, Fairfield, Ohio 45014.

A capillary GC/MS interface has been designed which combines most of the useful functions of traditional high flow packed column GC/MS interfaces as discussed by McFadden (*1*) with the advantages of direct insertion GC/MS. The following experimental section is a description of the methods used to evaluate the performance of such a device as a practical GC/MS interface. In the theoretical sections that follows the validity of these methods is demonstrated and the theoretical significance of the experimental data is discussed. The nature of the material has dictated this reversal of order from the norm. However, sufficient theory is presented along with the experimental data so that this section may be understood with minumum reference to the theoretical section.

Since the transition flow equations apparently do not explain the experimental data, an effort is made to distinguish between the experimental interface and a similar device for which these equations would apply.

EXPERIMENTAL SECTION

A simplified diagram of the interface is shown in Fig. 1. The length of the MS transfer capillary is equal to L. The column exit position (CEP) is the depth of insertion measured from the orifice of the MS transfer capillary. The withdrawn position is noted by a negative CEP. The sum of the MS flow rate Q_{MS} plus the flow to the separator vacuum (SV) system Q_{SV} is equal to the GC mass flow rate Q_{GC}. The GC column head pressure is P_i. The GC column exit pressure is P_e. The interface cavity pressure or

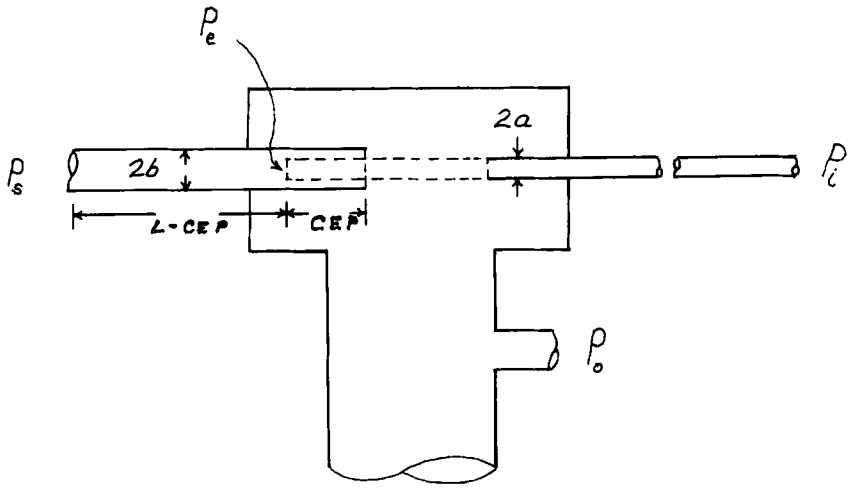

FIG. 1. Simplified diagram of the experimental GC/MS interface (not to scale).

separator exhaust pressure is P_o and the MS source pressure is P_s. The outside diameter of the GC column is $2a$; the inside diameter of the MS transfer capillary is $2b$. When the GC column is withdrawn from the MS capillary, $P_e = P_o$.

The percent carrier gas transmission (CPT) through the interface, assuming molecular flow conditions, is given by

$$\text{CPT} = \frac{100}{1 + C_{\text{SV}}/C_{\text{MS}}} \tag{1}$$

Using the Knudsen equations (*2, 3*) for the molecular flow conductance of long circular and annular columns (C_{MS} and C_{SV}), and assuming the P_e is always much larger than either P_o or the MS source pressure P_s, this becomes

$$\text{CPT} = \frac{100}{1 + (A - 1)(A^2 - 1)(L\text{-CEP})/(\text{CEP})} \tag{2}$$

where $A = a/b$, $A < 1$.

The assumption $P_e \gg P_o$ or P_s obviously breaks down for very short columns. For this reason there will be a short CEP interval near such extreme position (CEP = 0 and CEP = 19) where CPT is not well defined. However, since CPT is well defined exactly at CEP = 0 and at CEP = 19, a continuous smooth curve can reasonably be assumed over these very short intervals. In any case, CPT is well defined over the rest of the curve, including the higher pressure intervals where the maximum deviation would be expected. The importance of this will become apparent in a later discussion of interface pressure.

It was determined by point-by-point calculation that the orifice contribution to the total impedance of a short column can be neglected in calculating the percent transmission through this particular interface. In any case it seems likely that the orifice correction has less significance in this configuration where only a slight change in cross-sectional dimensions is involved in each case. Point-by-point calculation of the CPT was thus avoided, and the relatively simple expression above could be obtained for CPT (from 0 to 100%) versus CEP (from 0 to L). In Fig. 2 this equation is plotted by using the dimensions for several commercially available fused silica capillary columns. Although the Knudsen semiempirical equations for molecular flow are apparently less accurate than the Clausing and Monte Carlo equations (*3*), even for long capillaries when the orifice correction is not used, the percent transmission curves should be sufficiently accurate since they depend only on the ratio of the conductances and thus

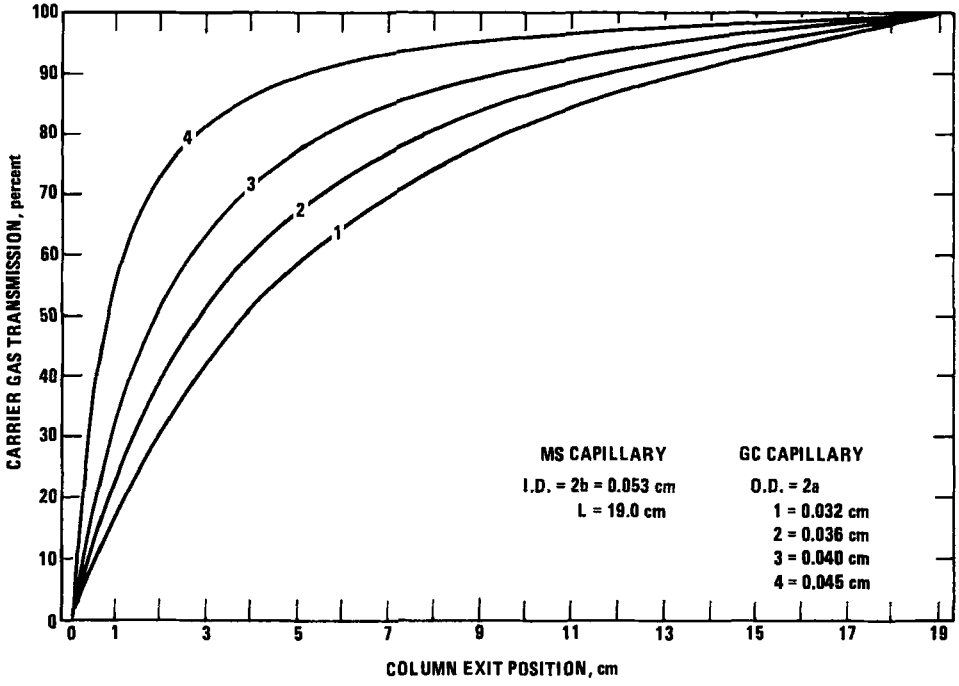

FIG. 2. Theoretical carrier gas percent transmission (CPT) under molecular flow conditions vs GC column exit position (CEP) for the experimental interface using four optional GC capillaries.

minimize the effect of the slight numerical error of the Knudsen molecular flow equations.

All of these experiments to be described were conducted using a Hewlett-Packard 5992 GC/MS instrument in which the isolation valve was drilled through to permit direct insertion of the fused silica GC column or the MS transfer column of the experimental interface. Neither column, however, could be inserted completely into the source because of the intervening repeller in this unusually designed source. The repeller has four symmetrically placed off-center holes for passage of carrier gas into the source. In these experiments the end of the MS transfer capillary is either touching or very close to the back surface of the repeller. This repeller can be easily replaced with one which has a tapered central hole which will guide an inserted slightly off-center fused-silica capillary directly into the source.

The interface is basically a modified Nupro 4BRK bellows valve in which a specially machined bar stock replaces the standard valve body and a special tapered Vespel valve stem replaces the standard stainless valve

stem. The sidearms fitted with standard swagelock fittings serve to connect and align the fused silica GC column and the MS transfer column across the valve gap. The MS transfer column is a 19-cm long section of commercially available extra wide bore fused silica capillary (0.053 cm i.d.) coated with a 1.65-μm methyl silicon film. A GC capillary (0.032 to 0.045 cm o.d.) can pass freely through the interface directly into the MS source. This is important since direct GC/MS becomes a convenient alternate mode of operation. It is also necessary for the proper operation and evaluation of the interface, as will be seen. A detailed description of an interface very similar to the experimental interface is given elsewhere, along with a simplified version attached directly to the MS source, and a more elaborate version with provisions for changing capillaries and the gap width (*12*, *13*).

The interface of the HP 5992 GC/MS is heated by the diffusion pump heater which is controlled at approximately 220°C. The actual temperature of the interface cannot be accurately controlled or monitored. The MS source is also not heated directly, and its temperature is estimated to be about 100°C. The GC end of the interface is in the GC oven (including about 3 cm of the MS transfer capillary). When the GC oven temperature is at 35°C and the CEP is 4 cm, the average temperature of the MS transfer capillary was estimated to be about 175°C and the average temperature of the SV capillary at 75°C.

The separator vacuum pressure P_o is measured by a capacitance manometer (MKS BHS 315-1, 4½ decades up to 1 torr) located in the interface sidearm connection to the separator vacuum pump which is an Edwards direct drive pump rated at 60 L/min for helium. The conductance of the connecting tubing between the pump and gauge was estimated to be 126 L/min (Z = 0.008 mpL) (Appendix 1). The manometer was zeroed by evacuating it below its minimum pressure (5×10^{-5} torr). The GC head pressure was measured by a mechanical gauge which was calibrated against a capacitance manometer (MKS-BHA 220-10K, 10,000 torr absolute).

Later experiments used this gauge directly. This capacitance manometer was zeroed by evacuating it below its minimum 1 torr pressure and also checked against atmospheric pressure as indicated by a standard mercury gauge.

Measurement of Percent Transmission through the Interface

The separator vacuum pressure P_o was used to generate percent transmission curves for the experimental interface. It was first determined that P_o is directly proportional to the undiverted GC flow rate over the entire experimental range by plotting the square of the GC head pressure P_i^2 versus the exhaust pressure P_o (Fig. 3), according to Eqs. (29) and (35)

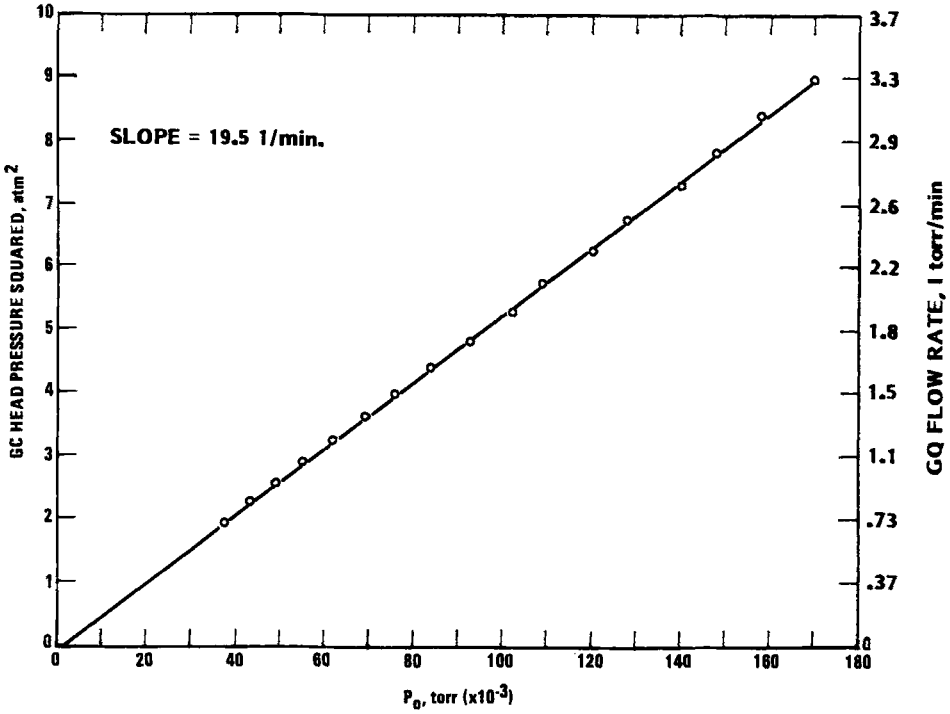

FIG. 3. Completely diverted (negative CEP) GC flow rate vs the separator vacuum exhaust pressure (P_o).

where P_o is the corrected exhaust pressure. This calibration plot also shows that the pumping speed at the gauge (S_X = 19.5 L/min) is constant over the 40 to 180 μ range and can be extrapolated to the origin (zero pressure, zero flow). This is apparently the limit for molecular flow conditions in this particular separator exhaust system (connecting tubes and pump) since the plot becomes nonlinear above 200 μ pressure.

In order to obtain the experimental percent transmission curves, the SV pressure P_o was plotted over the entire CEP range from −0.6 to 19.0 cm for four different GC flow rates (0.64, 1.1, 1.6, and 2.7 sccm). The CEP was measured from a reference "white-out" mark on the GC column to the end of the 1/16 in. nut for the ferrule sealing the column. Since only a very slight pressure on the ferrule was required to seal the column, the CEP could be changed with only a slight disturbance of the pressure each time. Every 5 cm a new reference mark was made on the column. The starting position for each experiment was CEP = 19 cm (fully inserted). Pressures were recorded at roughly 1 cm intervals as the GC column was

withdrawn from the interface. These results are shown in Fig. 4. The values of P_o for each experiment at a different GC flow rate are plotted against CEP by connecting the experimental points by straight lines. In the table in the upper part of Fig. 4, relative values of the GC flow rate (and P_i^2) are compared to the relative values of P_o for the undiverted (100%) GC flow and to the average relative values of P_o at successive column positions across the entire CEP range.

In addition to confirming that P_o is proportional to the GC flow rate as demonstrated in the previous experiment, this experiment shows that P_o is proportional to the SV (and MS) split flow over a wide range of GC

	GC HEAD PRESS. (P_i), atm	P_i^2	CALCULATED GC FLOW RATE, sccm	CALCULATED RELATIVE FLOW RATES	EXPERIMENTAL RELATIVE EXH. PRESS. (100% GC FLOW)	AVG. REL. EXH. PRESS. OVER SPLIT RANGE	STD. DEV. OVER SPLIT RANGE
A	2.36	5.57	2.67	1.000	1.000	1.000	–
B	1.82	3.31	1.60	0.594	0.607	0.613	1.49
C	1.49	2.22	1.06	0.399	0.432	0.440	1.24
D	1.16	1.34	0.64	0.241	0.248	0.254	1.55

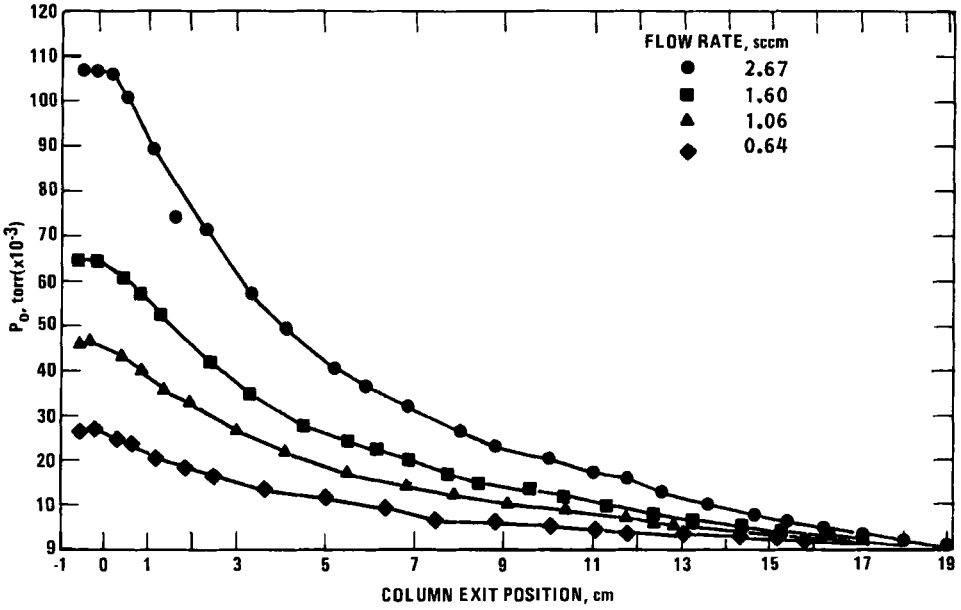

FIG. 4. Exhaust pressure in the separator vacuum line as measured by a capacitance manometer (P_o) vc GC column exit position (CEP) at four different GC flow rates.

flow rates as well. The comparisons were made exactly at each 1 cm mark of the plot across the entire range. The standard deviation indicates the good agreement for each experiment. The assumption was then made that the percent transmission to the MS (CPT) is zero at negative CEP values (GC column withdrawn for the MS transfer column) and 100% at full insertion (19 cm CEP). On this basis the CPT was calculated for each experimental CEP point. The resulting curves were compared to the theoretical molecular flow transmission curve (Fig. 5). A noise level which later proved to be the result of mechanical vibration limited the precision of P_o gauge readings to approximately 1%. It was later determined that the noise level could be reduced to very insignificant levels by mechanically stabilizing the gauge head. However, it is likely that the accuracy of the method of measuring the CEP is the limiting factor for these data rather than the pressure readings. The CEP can be measured very accurately if a reference marker is included in the original construction of the interface.

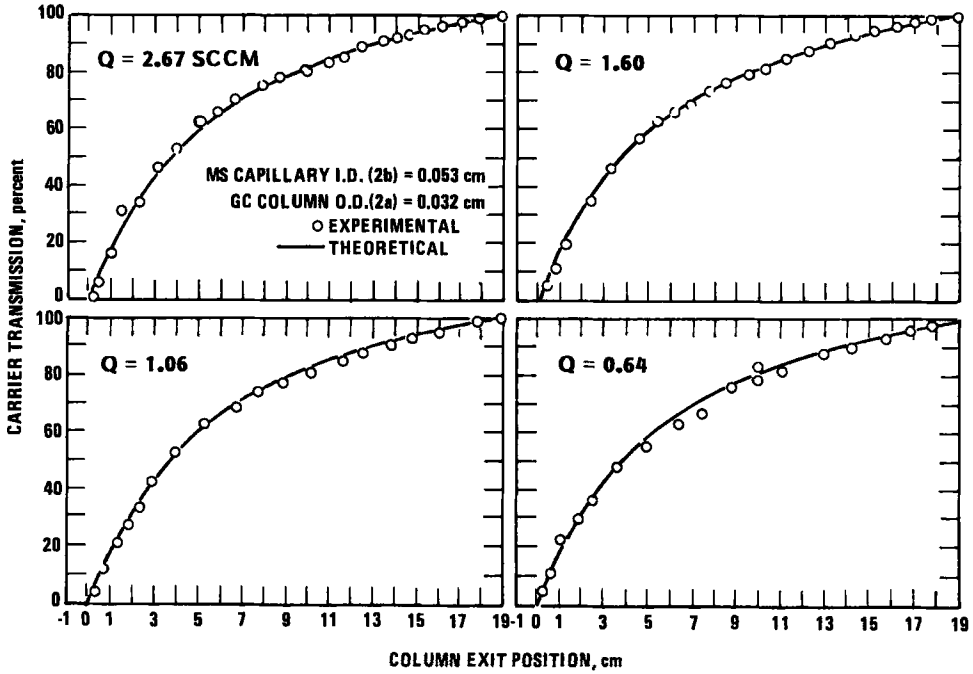

FIG. 5. Experimental CPT vs CEP curves for four different GC flow rates compared to the theoretical molecular flow curve.

These curves demonstrate that P_0 can also be used to accurately measure the CPT, and that the CPT is constant at a given CEP up to at least 2.7 sccm for these particular interface capillaries. The standard deviation of the raw data (Fig. 4) applies to these curves as well. The good agreement with the theoretical curve is also apparent from these plots.

In Fig. 6, successive experimental CPT vs CEP curves were obtained by using GC columns with outside diameters of 0.032 and 0.036 cm. Both of these 30-m long columns had an i.d. of 0.025 cm. The difference in the outside diameters is apparently the result of the difference in the thickness of their outer polyimide coating. The agreement with the theoretical molecular flow curves is not quite so good here as for the previous set of experiments with different flow rates, but the difference is probably still within experimental limits. This good agreement with the molecular flow curves even at the higher flow rates was unexpected. The significance of this will be discussed further in the theoretical section.

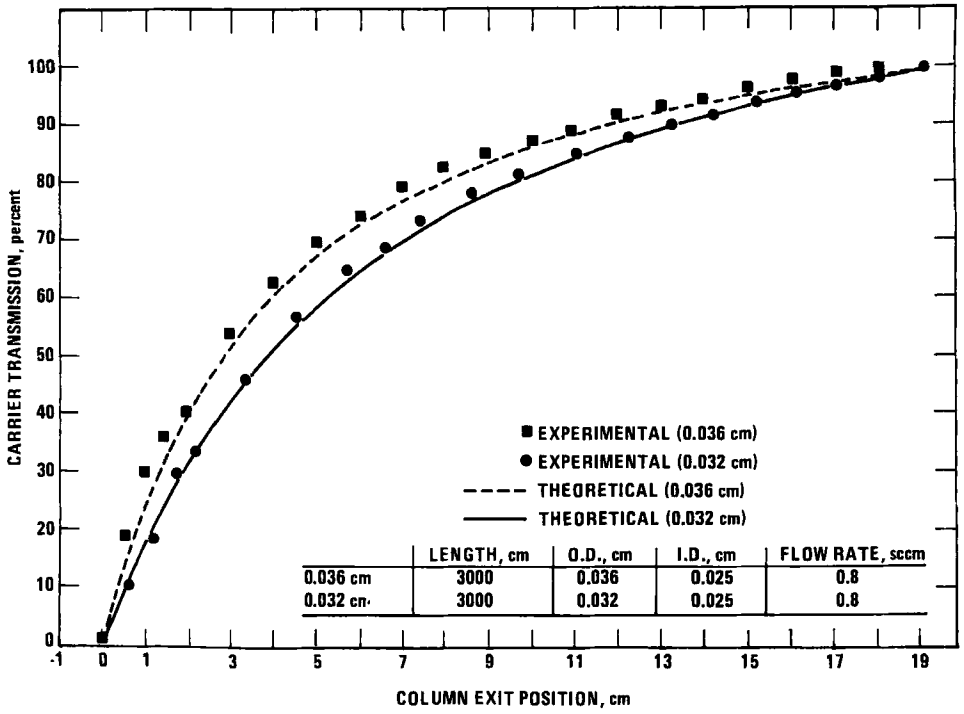

FIG. 6. Experimental CPT vs CEP curves are compared to the theoretical molecular flow curves. Two different GC columns with different outside diameters are used.

Experimental Measurement of Sample Enrichment

The enrichment factor may be defined simply as the ratio of the sample percent transmission through the interface to the carrier gas percent transmission as given by

$$E = \text{SPT/CPT} = (r/r_{100})_s/(r/r_{100})_c \quad (3)$$

where the s and c subscripts refer to the MS detector response for the sample and carrier gas, and the 100 subscript designates the response at 100% flow.

More conveniently:

$$E = (r_s/r_c)_x/(r_s/r_c)_1 = R_x/R_1 \quad (4)$$

where R_x is the measured sample to carrier gas response ratio at any experimental CEP position and R_1 is the same ratio at a CEP where the enrichment factor is assumed to be unity such as for a direct connection when CEP = L = 19 cm. A practical limitation to the use of this reference is that the measurement cannot be made (with the HP5992) for most useful GC flow rates since the source pressure will be too high.

Another useful reference point where E should be unity occurs when the GC capillary is completely withdrawn from the MS transfer capillary to a point beyond the range for any GC flow effects. Since the CPT is very low at negative CEP positions (0.1%), this method is applicable to high GC flow rates. The disadvantage is that the MS response may be so low for reasonable sample concentrations that selected ion monitoring (SIM) analysis is required and even then the percent error may be rather high compared to that at higher CEP positions.

Both continuous flow analysis of a gas mixture and conventional GC analysis of an alkane series were used in these experiments. The relatively simple continuous gas flow analysis was used both as a convenient alternate method and also as a way to eliminate condensation and other peak spreading effects which could effect the conventional GC analysis. For these preliminary experiments a 3% butane in helium mixture was used (a 5-component gas mixture will be used for future experiments). This is compared to the approximately 3×10^{-5} volume percent concentration within the GC peak for the 50 ng/μL alkane sample used.

If r_s and r_c could be measured simultaneously over the entire CEP range, a very accurate value of E as a function of CEP independent of pressure, source tuning effects, or drift in the electron multiplier gain could be determined. However, the range of the multiplier output cannot cover the entire split range for both sample and carrier ions (58 and 4 amu) under the same SIM conditions (dwell time and multiplier gain). This requires

that separate runs must be made; one for the sample response and one for the carrier gas response, with optimized SIM parameters for each. The values of R_x and R_1 may then be meaningless by themselves, but their ratio within the experimental probability of making two or more consecutive runs under nearly identical conditions gives an accurate value for the dimensionless enrichment factor. Each of the experimental points in the following graphs represent the average of two or more analyses. In the case of conventional GC analysis, r_s is a peak area response count and r_c is a baseline displacement response count. For continuous flow gas analysis, both values are baseline displacement counts.

In Fig. 7 the results are shown for the continuous flow SIM analysis using two different size GC columns at two different flow rates. In the top graphs the log of the MS detector response counts for 4 and 58 amu are plotted against the CEP. In the bottom graphs the enrichment factor E is plotted against CEP. E was calculated using the reference ratio R_1 obtained at the most negative CEP value (furthest withdrawn position). In both cases there is a sharp increase in the enrichment factor at the insertion point (CEP = 0).

For the wide bore column, where the annular space ($b - a$) is smaller, the GC flow rate is higher, and the angle of flow diversion is sharper, a sharp peak occurs just at CEP = 0. For these conditions the maximum depth of insertion is CEP = 3 mm, which corresponds to the maximum flow rate to the MS for the HP 5992. Above this flow rate the MS response is unstable and not reproducible. Since the sample yield ($Y = E \times \text{CPT}$) exceeds 100% at the highest CPT, the accuracy of this E factor must be questioned, at least on this basis, although the accuracy of the CPT value has already been demonstrated. Simultaneous enrichment effects in the MS source itself is a possible answer. Only a slight enrichment effect in the source ($E = 1.6$) would be required to explain the experimental results. In the first curve in Fig. 7 the maximum experimental enrichment factor (5.5) is compared to that for the maximum possible velocity enrichment ($E = 3.8$ for C_4 and helium). In the second curve the experimental enrichment factor (17.5) far exceeds any possible velocity enrichments effects. It can be shown by calculation that for all these experiments the theoretical velocity enrichment factor (E_V) is insignificant (maximum values less than 2) compared to the experimental values observed.

Velocity molecular enrichment (E_V), whose maximum possible value is given by $E_V = (M_s/M_c)^{1/2}$, where M_s and M_c are the sample and carrier molecular weights, is explained in some detail as it applies here in the theoretical section. This is the type of molecular enrichment that occurs in devices such as the Bieman Watson separator which was used for high flow packed volume GC/MS (*1*).

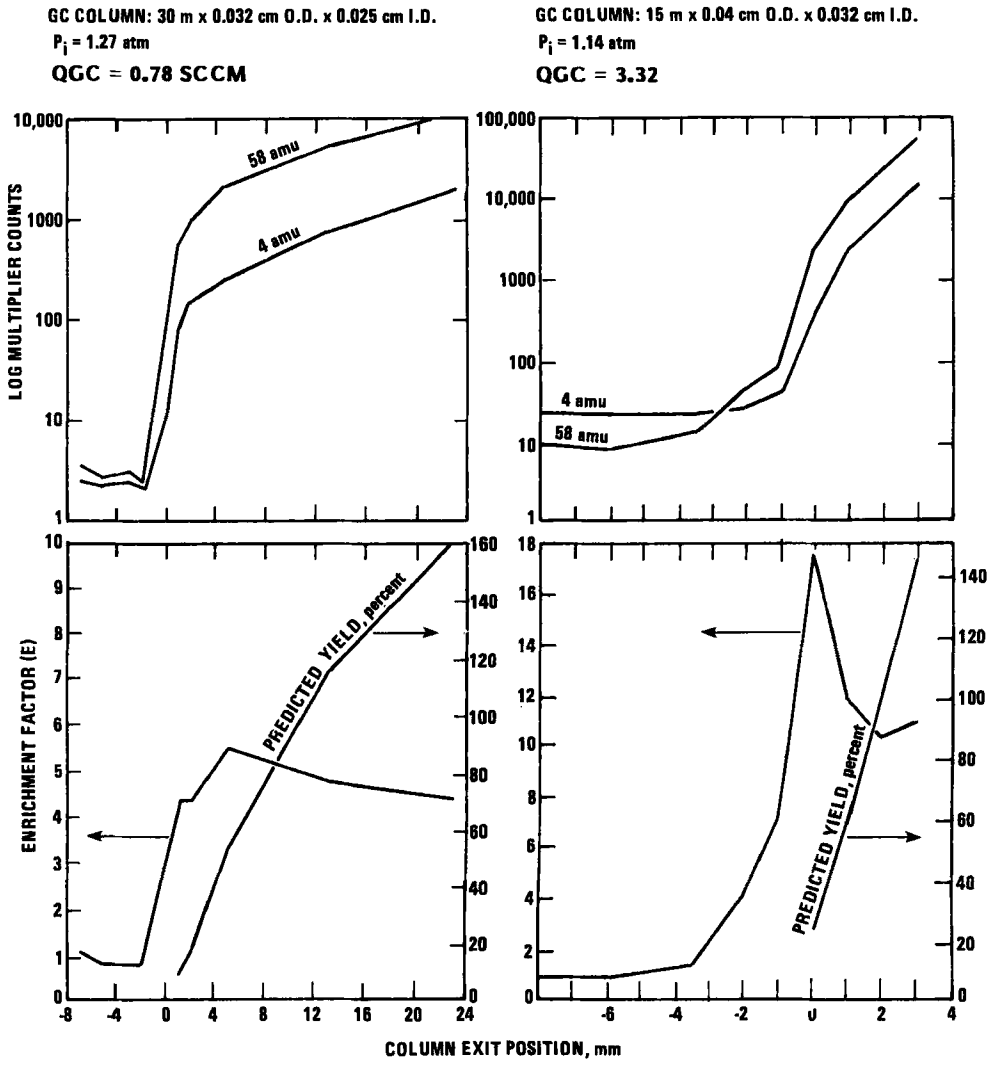

FIG. 7. The results of a continuous flow SIM analysis of 3% butane in helium, using two different GC columns at two different flow rates. In the upper figures the sample and carrier gas responses (r_s and r_c) are plotted against the CEP on a log scale. In the lower figures the enrichment factor (E) and percent yield is also plotted against the CEP. The scale on the right indicates the predicted percent yield.

The results are shown in Fig. 8 for an experiment in which the first analysis with the narrow bore column (0.025 cm i.d.) is repeated using a slightly lower flow rate over the entire CEP range. At this low flow rate (0.8 sccm) the entire GC effluent can be tolerated by the MS. The sharp increase in E shown in the bottom graph, which occurs just at CEP = 0, is not as large as before. Whether or not the slight drop just in front of the orifice is real can only be determined with repeat experiments. An accidental loss of pressure in this region is suspected.

There is a gradual decline in E as the CEP (and the CPT) increases (Fig. 8c). This is expected since the yield cannot exceed 100%. The value of E at CEP 19 is approximately 1, as expected. However, there are obvious discrepancies here. In Fig. 8(a) the percent multiplier response (compared to the CEP 19 response) is plotted against the CPT for both butane and helium. The response in both cases is obviously nonlinear with source pressure. This is also shown by the CPT curve in Fig. 8(b) where the same data are plotted in a different way. The change in the MS response for both butane and helium is shown to be nearly linear with the change in CEP as compared to the change predicted by the CPT curve. These graphs explain the decrease in sensitivity that is apparent from the decrease in the signal-to-noise ratio shown later in Fig. 10 for the chromatograms at CEP 4 compared to CEP 19. The only apparent variables are the partial pressures of the two gases in the source and the GC column position within the MS transfer column. Apparently there is some change in the ionization efficiency of the electron impact process as the CEP is changed. This suggests the existence of a sharp pressure gradient within the source, although the repeller barrier apparently prevents any direct flow stream effects. It will be important to determine the effect of removing the repeller barrier so that the GC effluent is exposed directly to the electron beam.

It is important at this point not to allow the much lower than predicted sensitivity indicated in Figs. 8(a) and 8(b) to obscure the potential advantages of molecular enrichment and the possibilities the data also reveal for increasing the sensitivity by means other than molecular enrichment, since the data are also significant as an indication of nonuniform gas flow through the source.

These molecular enrichment experiments were repeated using conventional temperature program GC/SIM analysis with an alkane series sample (C_8–C_{17}), 50 ng/μL/component with approximately 1 μL injections (the response is normalized to 1.0 μL in all cases). The GC column is the same wide bore column as in the second set of curves in Fig. 7. The result of a typical experiment is shown in Fig. 9. Again, each plotted point represents the average of two or more experimental points. The helium response was measured in a separate run under different SIM conditions at retention

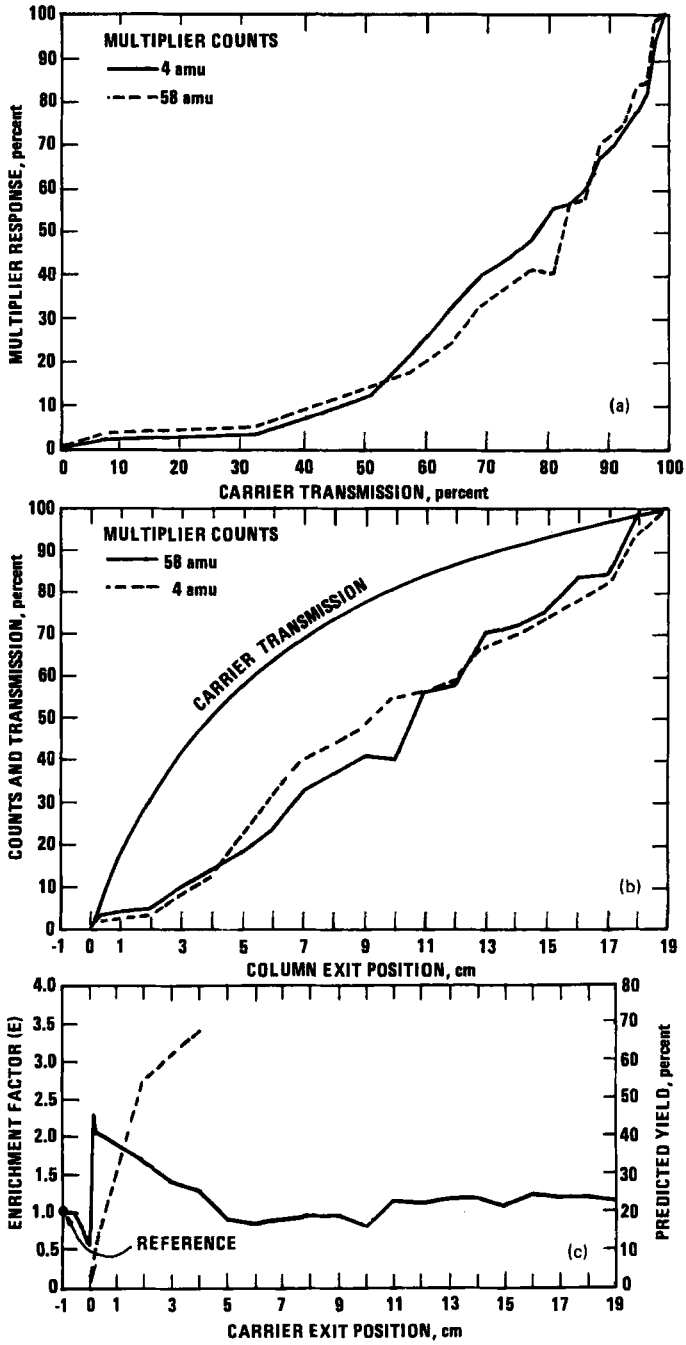

FIG. 8. Continuous flow SIM analysis of 3% butane in helium. GC column: 30 m × 0.32 mm o.d. × 0.25 mm i.d. Q_{GC} = 0.8 sccm. (a) Percent multiplier response (mass 4 and 58) vs CPT. (b) CPT and multiplier response vs CEP. (c) Enrichment factor (E) and percent yield vs CEP.

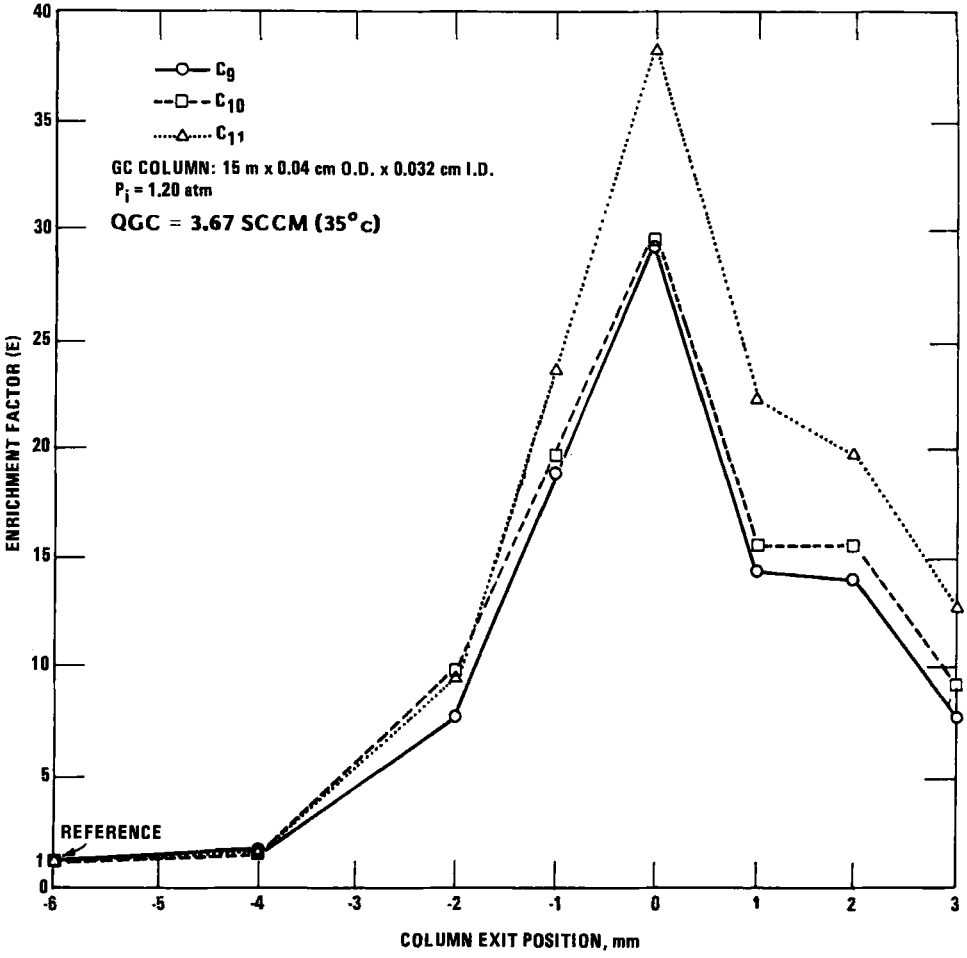

FIG. 9. The enrichment factor (E) vs the column exit position (CEP) in millimeters for a conventional GC analysis of alkanes.

times corresponding to each alkane peak (Appendix 2). The SIM ion was 71 amu for the alkanes. Mass 71 was chosen because of the significantly lower relative response of the hexane solvent compared to the higher alkanes.

Only the values for C_9 through C_{11} were used since some noticeable peak broadening occurred for the higher alkanes. The apparent reason for this is that the temperature of the GC end of the interface lags behind the column temperature by about 60 during the analysis. This produces sample

condensation on the metal interface surface when the GC column is withdrawn to negative CEP positions, which results in low and nonreproducible r_s reference values for higher molecular weight alkanes. Reproducible response and the absence of peak broadening is a reasonable assurance that appreciable sample adsorption did not occur for the lower alkanes (C_9–C_{11}), for which the experimental enrichment factors were obtained. This low interface temperature is easily avoided in most GC/MS systems by independent interface temperature control. This problem is avoided entirely by the continuous flow trace gas analysis described above. Again, the high GC flow rate limits the maximum CEP position for this experiment.

There is a sharp peak in the enrichment factor curve just as CEP = 0 occurs for each alkane. Data from the entire mass range (C_8–C_{17}) are needed to clearly establish the mass dependence of the enrichment factor. Obviously, further experiments are required in order to confirm the existence of an enrichment factor directly in terms of the true percent yield. The reason for the simultaneous nonlinear 4 and 58 amu detector responses versus pressure with increasing CEP (Fig. 8) must be established. However, the data as presented here can stand on their own merits. A sharp increase in the relative response to the two molecular species just at the point of maximum flow reversal is compelling evidence in itself that the observed enrichment factor is real. It will be very useful to differentiate experimentally between velocity enrichment E_V and a second much larger enrichment factor E_m which is due to momentum effects. However, E_V can be related to molecular weight as noted above. If the enrichment factor can be determined under conditions where only velocity enrichment (E_V) occurs and also under molecular flow conditions when E_V is equal to zero, the values of E_V for an alkane series may be used to calibrate the analytical method for the measurement of the unknown factor E_m. Under the conditions of the experiment, E_m cannot be explained in terms of the conditions required for a conventional jet separator (*1*).

Chromatography

A comparison of the chromatograms in Fig. 10 shows that the interface can be used to increase the chromatographic efficiency over that obtained with a direct connection using the Hewlett Packard 5992 GC/MS. The chromatograms are for a 30 m × 0.252 mm DB5 column with a 0.25-μm film thickness. The column temperature was held at 35 for 3.5 min, then programmed to 300°C at 16/min. The manufacturer's specifications are: $N = 126 \times 10^3$ total theoretical plates and separation number $Tz = 38.7$. The sample is a standard polarity test mixture at 50 ng/μL/component

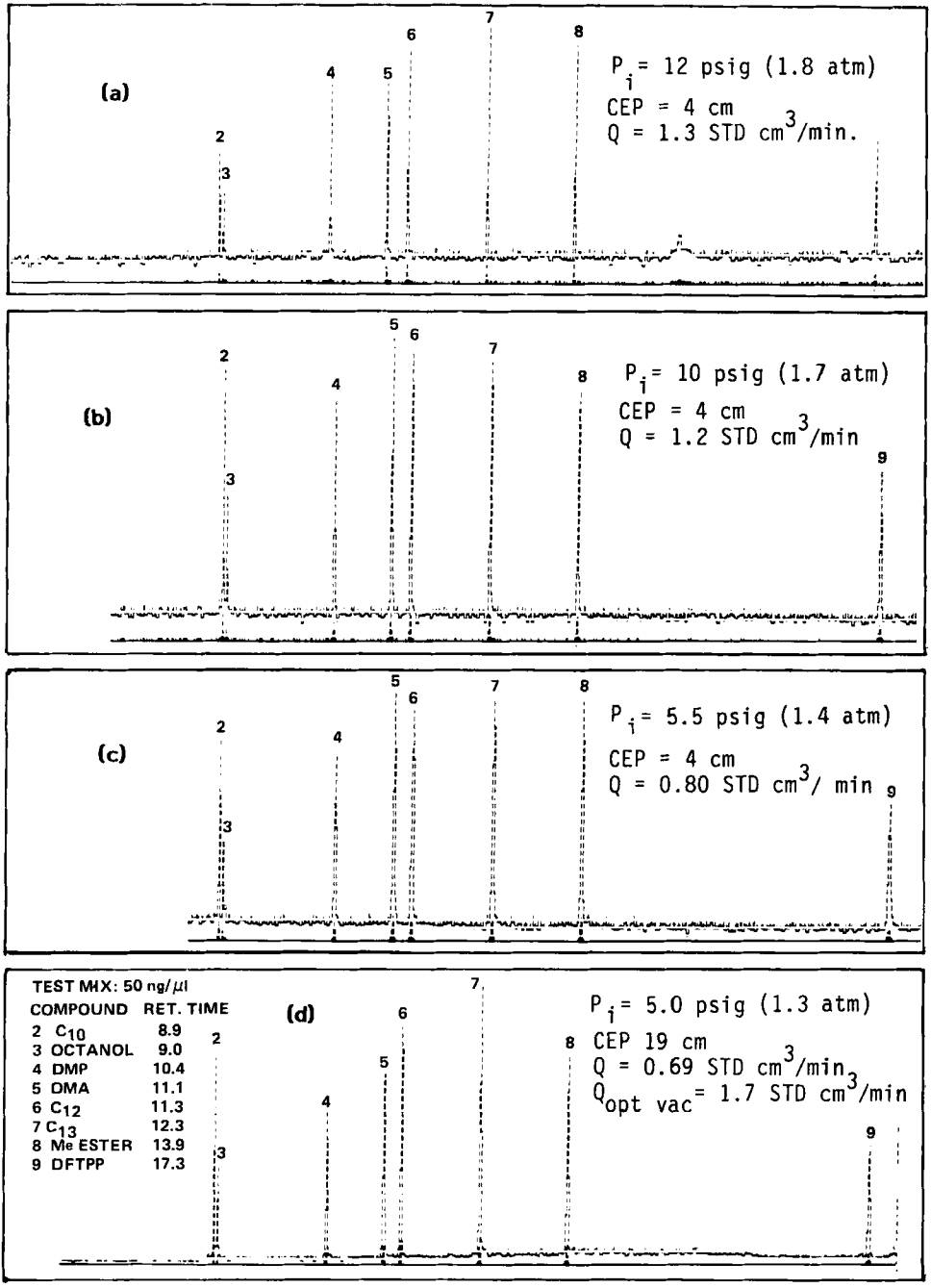

FIG. 10. A comparison of the GC efficiency at 4 cm CEP (a, b, c) at three different flow rates, with the GC efficiency at 19 cm CEP (d) using the maximum flow rate for a direct connection. The GC column is a DB-5 (30 m × 0.252 mm) with a 0.25-m film thickness. The temperature program is 35°C (3.5 min) to 300°C at 16°C/min.

with 1 μL injections. Flow rates are 0.80, 1.2, and 1.3 cm, respectfully, for the 4-cm CEP runs and 0.69 sccm for the 19-cm CEP run. The optimum head pressure P_i for vacuum outlet GC is given by the equation (7)

$$P_i^2 \text{ (opt vac)} = (72PN\eta D)/a^2 \tag{5}$$

where P = atmospheric pressure; N is the total number of theoretical plates; η, the viscosity, equals 232×10^{-12} atm·s for helium at the retention temperature (400 K) (Appendix 3); D (0.304 cm^2/s for helium and C-12) is the binary diffusion coefficient of a component in the mobile phase at atmospheric pressure; and a is the column radius. The optimum inlet pressure is 2.09 atm. The optimum GC flow rate (1.7 sccm) is obtained by using Eq. (29) for the mass flow rate through a column under vacuum exhaust conditions.

A clear demonstration of the advantage in being able to use the optimum flow rate is seen in the decrease in peak width as the flow rate is increased for each chromatogram.

Finally, in order to use the experimental separator as a practical capillary GC/MS interface, the GC flow rate (or linear velocity) is first adjusted to its optimum value according to Eq. (5) for optimum GC head pressure. Then the position of the GC column in the interface (CEP) is adjusted to the maximum allowable position (CEP) according to the maximum flow capacity of the particular MS and the CPT versus CEP curve. Since the MS pressure will be the limiting factor, this will also give the maximum yield or sensitivity.

For ordinary capillary GC/MS, the high enrichment factor obtained at CEP = 0 is not needed (and cannot be effectively utilized because of the low yield).

The expected performance of the interface using high, packed column GC flow rates will be discussed in a future paper.

THEORETICAL SECTION

The transition region between viscous flow and free molecular flow in circular tubes is defined by the following empirical relationships developed by M. Knudsen. The application of these relationships to the interface capillaries was adapted from the discussion of transition flow by Lafferty and Dushman (*3*) as shown in Eqs. (6)–(16). Equation (6) defines the limits to the transition region in terms of the ratio of mean free path to the radius of the column.

$$0.01 < L_a/a \leq 1 \tag{6}$$

where L_a is the average mean free path of the gas molecules flowing through a circular tube of radius a. L_a may be conveniently determined at a given pressure by using a reference value L_1 calculated according to kinetic theory at 1 micron pressure (L_1 for helium at 25°C is 14.7 cm).

For the MS transfer capillary of the interface:

$$L_a = L_1/P_a \tag{7}$$

where P_a is the average pressure along the tube in microns.

Again assuming that P_e is always much greater than P_o or P_s, Eq. (7) becomes

$$L_a = 2L_1/P_e \tag{8}$$

A further empirical relationship was established by Knudsen for transition flow:

$$F = F_v + ZC \tag{9}$$

where F is the actual or transition flow conductance and F_v and C are the viscous and molecular flow conductances, respectively.

Z is a third empirical definition by Knudsen which is a function of the pressure in the tube, the temperature, the tube radius, and the viscosity of gas which can be reduced to a function of the inverse Knudsen number (a/L_a) for a long cylindrical tube. In terms of the MS transfer capillary and the GC column exit pressure P_e,

$$Z = \frac{1 + 2.51(a/2L_1)P_e}{1 + 3.10(a/2L_1)P_e} \tag{10}$$

When the pressure P_e is high, Z approaches the constant value 0.810 and the molecular flow term in Eq. (9) becomes a small addition to the viscous term which is proportional to the pressure. At low pressures, Z becomes equal to unity and the transition conductance F approaches the molecular flow conductance since F_v also becomes small.

Equation (9) can be expressed in a more convenient form:

$$F/C = F_v/C + Z \tag{11}$$

From the equations for F_v and C for long circular tubes, an expression for their ratio can be obtained:

$$F_v/C = 3/16(a/v_a\eta)P \tag{12}$$

where a is the tube radius and v_a and η are the molecular velocity and viscosity, respectively, as defined by kinetic theory.

Using the ideal gas law and the equations for v_a and η, this equation can be reduced to

$$F_v/C = 0.147a/L_a = 0.147(a/2L_1)P_e \tag{13}$$

Substituting in Eq. (11) gives

$$\frac{F}{C} = (0.147a/2L_1)P_e + \frac{1 + 2.51(a/2L_1)P_e}{1 + 3.10(a/2L_1)P_e} \tag{14}$$

If Z, which varies between 0.810 and 1, is assumed to be 1, a useful linear relationship is obtained for this ratio as a function of the column exit pressure P_e:

$$F/C = kP_e + 1 \tag{15}$$

where $k = 0.147a/2L_1$. The decimal place depends on whether P_e is in microns, as above, or in torr.

The mass flow rate through the MS transfer capillary can be determined from $Q = PF$ by using Eq. (15).

$$Q = kCP_e^2 + CP_e \tag{16}$$

Transition Flow Characteristics of the Interface

A more general expression for CPT as a function of interface conductance applicable at any pressure is given by

$$\text{CPT} = \frac{100}{1 + F_{SV}/F_{MS}} \tag{17}$$

where F is the transition flow conductance.

Equation (17) may be written as

$$\text{CPT} = \frac{100}{1 + (C_{SV}/C_{MS})K} \tag{18}$$

where K is given by the following equation if we assume for the time being that both the MS and SV capillaries are separate circular capillaries:

$$K = \frac{1 + k_{SV}P_e}{1 + k_{MS}P_e} \tag{19}$$

where k_{SV} and k_{MS} are the respective constants from Eq. (15) for the interface columns.

At low molecular flow level pressures, K equals unity since the second term in both the numerator and denominator becomes small compared to 1. At higher pressures, K will equal unity only if k_{SV} and k_{MS} are equal to each other. If the internal diameters of the MS and SV capillaries are different, K will vary between unity and a minimum value $K_{min} = k_{SV}/k_{MS}$ as the pressure increases from molecular to viscous flow levels as shown in Fig. 15.

The Knudsen Splitter

It will be useful for several reasons, which will become more apparent as we go along, to develop the application of the pressure factor K initially in terms of a hypothetical circular tube splitter which is equivalent to the experimental separator, at least under molecular flow conditions. A functional diagram of this device, which will be referred to as the Knudsen splitter, is shown in Fig. 11. The symbols in Fig. 11 are equivalent to those used for the experimental separator in Fig. 1. It will be useful for comparison purposes to apply the relation (L − CEP) + CEP = L for the total length of the separate MS and SV capillaries for the Knudsen splitter as well, although it may not be convenient to do this in practice.

A plot of the ratio of the actual or transition flow conductance to the molecular flow conductance as a function of the interface pressure P_e (Eqs. 14 and 15) is shown in Fig. 12 for both the MS and SV capillaries of the Knudsen circular tube splitter. The molecular flow transmission curve (Eq. 2 and Fig. 2) is the same as for the experimental interface, since the radii (a^*) of the optional circular SV capillaries (Eq. 20) were chosen so that the conductance (C) of these capillaries would be the same as for the corresponding annular capillaries of the experimental interface.

$$a^* = [(b^2 - a^2)(b - a)]^{1/3} \tag{20}$$

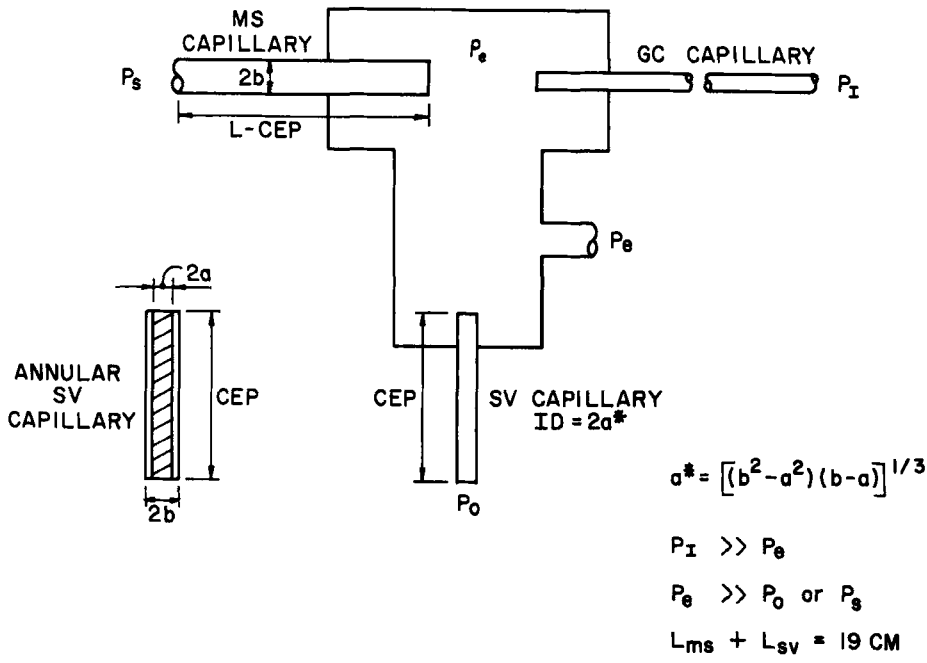

FIG. 11. Simplified diagram of the Knudsen splitter.

The large and small dimensions of an annular capillary are given by b and a, respectively (Appendix 4).

These F/C curves exhibit a minimum which can be noted experimentally and occurs when the mean free path is greater than the radius of a tube but less than its length (*3*). A detailed theoretical explanation is given by Pollard and Present (*4*).

The calculated slope ($k = 147a/2L_1$) is given for the linear section of each curve (Eq. 15) for both the MS and optional SV capillaries. The corresponding value for K_{min} is also noted for each SV capillary.

The Experimental Separator

A similar set of curves is shown for the experimental interface in Fig. 13, in which the method just described to define the transmission characteristics of the circular splitter was applied directly to the more complicated geometry of the experimental interface. The values of K and K_{min} were determined as before by using the same MS capillary (A) and the corresponding annular SV capillaries resulting from the use of the same GC capillaries as in Figs. 2 and 12. An expression for the ratio of the

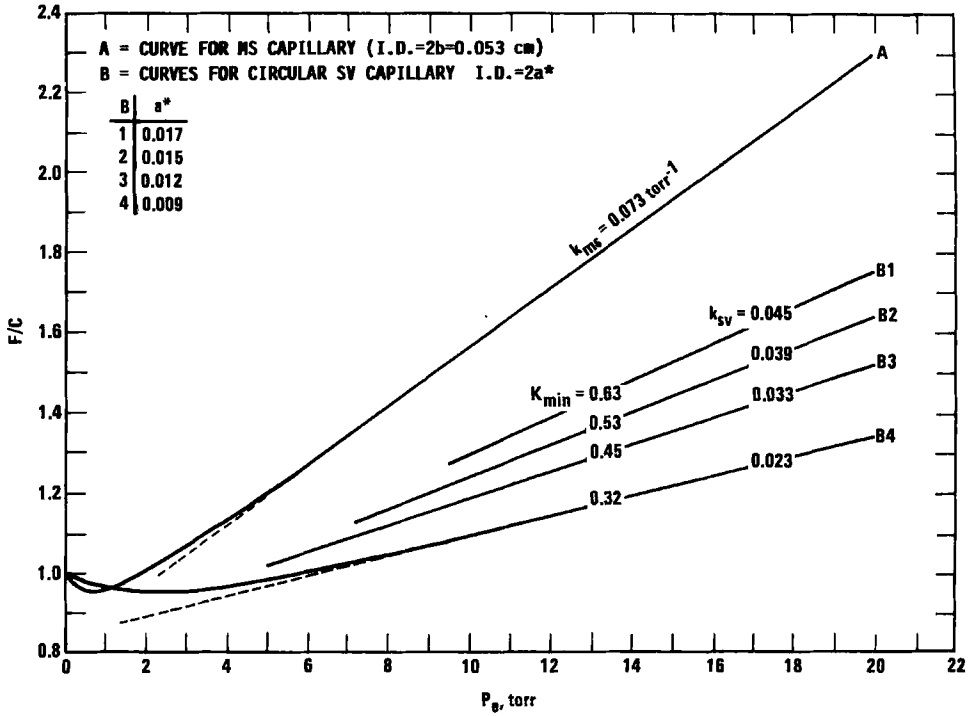

FIG. 12. Predicted ratio of transition flow conductance to molecular flow conductance (F/C) vs the column exit pressure P_e for a Knudsen circular column splitter (Fig. 11) whose molecular flow transmission characteristics should be the same as for the experimental interface. A comparison is shown between the curves for the circular MS capillary (A) and the hypothetical SV capillaries (B) with i.d. equal to $2a^*$ (Eq. 20).

viscous conductance to the molecular flow conductance for annular tubes corresponding to Eq. (12) for circular tubes is obtained. Then, in the same manner as before, a straight-line relationship for the ratio F/C is obtained:

$$\frac{F}{C} = \frac{147}{2L_1}\left[\frac{b^2 + a^2}{b - a} - \frac{b + a}{\ln (b/a)}\right]P_e + 1 \qquad (21)$$

Although there is apparently no corresponding value defined by Knudsen for Z in terms of the cross-sectional dimensions of annular tubes, it seems apparent from the plot in Fig. 13 that at least for these low values of k (from 0.019 to 0.007) the assumption that Z equals 1 is just as appropriate

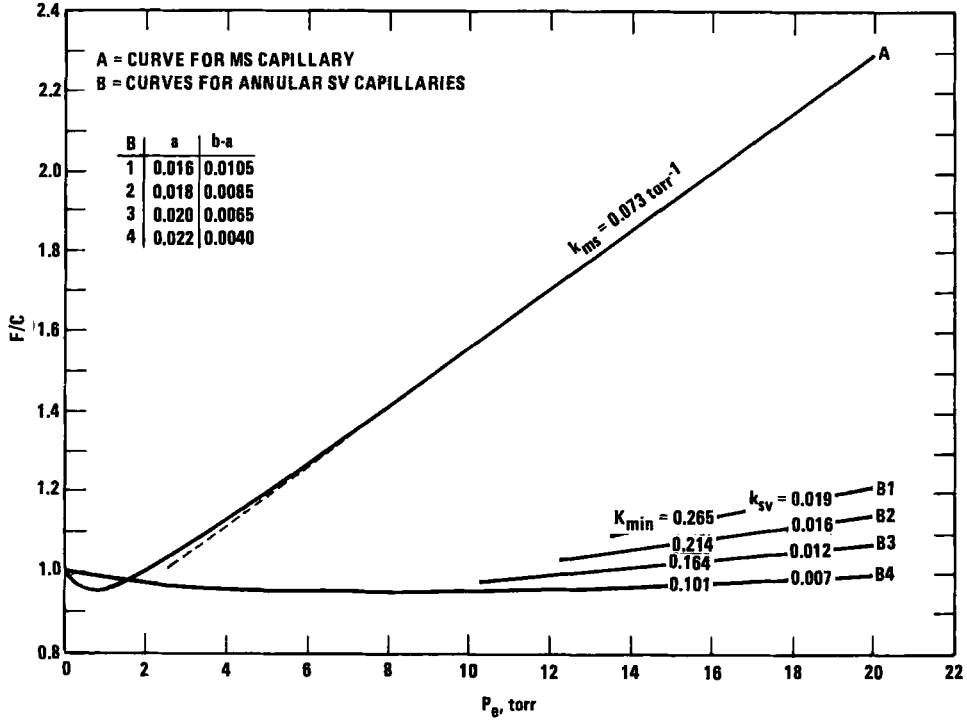

FIG. 13. Predicted ratio of the transition flow conductance to the molecular flow conductance (F/C) vs the GC column exit pressure (P_e) for the capillaries of the experimental interface.

and useful as in the case of circular tubes. In either case, the F/C ratio is accurately defined by these equations except in the narrow interval ($kP \approx 1$) as shown in each plot.

The fact that there may be an error as high as 14% in this narrow region due to the $Z = 1$ approximation as shown by the dotted line in each plot does not affect the most important implications of these plots for percent transmission. Only the CPT/CEP plot at the lowest flow rate should be affected (Fig. 5). However, it will be very useful to examine experimental data in this region very closely for the presence of this same degree of uncertainty as an indication of the presence of this same transition flow effect in the experimental interface.

If Eq. (21) is compared to Eqs. (13), (14), and (15), it can be seen that the term in the brackets should represent the characteristic dimension of an annular column just as the radius represents the characteristic dimension of a circular column. The characteristic dimension is defined as the average lateral distance a molecule must travel before striking a wall surface. By

inspection, it would be expected that the characteristic dimension of an annular capillary would be some fractional value greater than $^1/_2$ of the annular space $(b - a)$. This is apparently true for small values of $(b - a)$, since it can be shown numerically that in this case the term in the brackets equals $(2/3)/(b - a)$ which includes the range of experimental values for $(b - a)$ reported here (Appendix 5). This yields a simplified form of eq. (21) for transition flow through annular columns.

$$F/C = (0.147/3L_1)(b - a)P_e + 1 \tag{22}$$

where $k_a = (0.147/3L_1)(b - a)$ compared to $k_c = (0.147/2L_1)(a)$ for circular columns.

At high pressures where the first term is large compared to 1 [and again, $(b - a)$ is small], Eq. (22) leads to the following simplified equation for viscous flow through an annular column:

$$F_v = (\pi/12\eta L)(b^2 - a^2)(b - a)^2 P_a \tag{23}$$

A numerical proof of Eqs. (22) and (23) over the range of the experimental conditions is given in Appendix 5.

Column Exit Pressure

It is apparent that the pressure at the end of the GC column, P_e, will vary considerably depending on the CEP.

Under molecular flow conditions:

$$P_e^* = \frac{Q_{GC}}{0.126V_a\,[b^3/(L - \text{CEP}) + (b^2 - a^2)(b - a)/(\text{CEP})]} \tag{24}$$

where P_e^* is defined only under molecular flow conditions. Q is the mass flow rate in L·torr·min^{-1}; v_a is the molecular velocity for helium in cm/s. The denominator is the sum of the MS and SV conductancies.

P_e^* is plotted against CEP for the four optional GC capillaries in Fig. 14(a). Since the conductance of both the MS and separator vacuum (SV) capillaries will increase with pressure under nonmolecular flow conditions, P_c^* as calculated by Eq. (24) gives a value much higher than the actual pressure for most capillary GC flow rates. However, it will be convenient to use the value of P_e^* in calculating the pressure at higher flow rates below. Values for the interface pressure (P_e) under transition flow conditions can be obtained from Eq. (16), which is accurate except in a very narrow region as discussed previously.

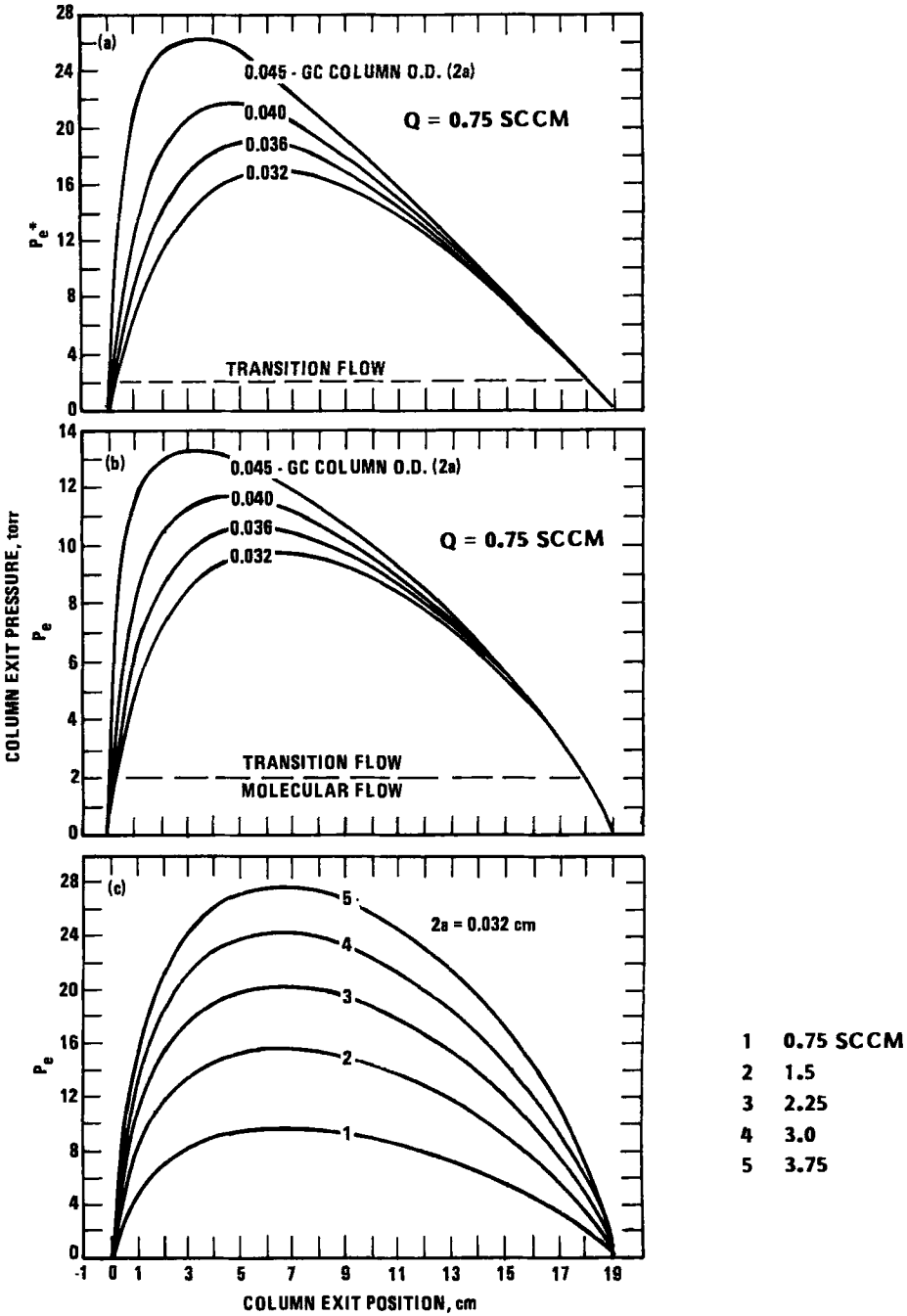

FIG. 14. GC column exit pressure (P_e) vs column exit position (CEP). (a) Assuming molecular flow conditions (P_e^*). (b) Under transition flow conditions. (c) For five different flow rates. The transition flow curves above were obtained by using Eq. (25) with $k = k_{MS} = 0.073$ torr^{-1}. A more accurate pressure vs CEP curve could be obtained by using $k_s = (C_{MS}k_{MS} + C_{SV}k_{SV})/(C_{MS} + C_{SV})$ which reduces to the simple average $k_s = (k_{MS} + k_{SV})/2$ at approximately CEP = 4.

Solving the quadratic equation and letting $P_e^* = Q/C$:

$$P_e = (\tfrac{1}{4}k^2 + P_e^*/k)^{1/2} - \tfrac{1}{2}k \tag{25}$$

where $k = 147(a/2L_1)$ for circular capillaries and the pressure is in torr.

P_e is plotted as a function of CEP in Fig. 14(b) by using P_e^* from Fig. 14(a) and assuming k is the same for both the MS and SV capillaries. In Fig. 14(c), P_e is plotted for several different flow rates.

The effects of the GC flow rate on the percent transmission through the interface can now be predicted on the basis of the Knudsen transition flow relationships. In the general case, Eq. (18) and (1) for transition and molecular flow, respectively, are identical except for the pressure factor K. Similarly for the experimental separator, Eq. 26 below and Eq. (2) are also identical except for the pressure factor K.

$$\text{CPT} = \frac{100}{1 + (A - 1)(A^2 - 1)\left[\dfrac{L - \text{CEP}}{\text{CEP}}\right]K} \tag{26}$$

In Fig. 15 the pressure factor K is plotted against the column exit pressure P_e for two of the optional SV capillaries from each interface (Figs. 12 and 13). It is apparent that in each case $K_{\min}$ has not been reached even at 100 torr. $K_{\min}$ defines the upper limit of the transition region in the interface. In Fig. 16, percent transmission curves (CPT vs CEP) are plotted for different values of K ranging from 1.0 down to 0.4 in 0.1 intervals using a GC capillary with an outside diameter of 0.032 cm. Using Eq. (25) where k is equal to k_s, a CPT-dependent value, and Eq. (19), new percent transmission curves similar to those in Fig. 2 may be constructed in a point-by-point manner which takes into account the effects of pressure above the molecular flow level at a given GC flow rate. However, for our purposes here it is sufficient to determine the maximum expected deviation from the molecular flow curve. This can be accurately determined by calculating K at the CEP where the maximum pressure occurs. The exact shape of the curve away from the maximum as it approaches the molecular flow curve is not so important.

In Table 1 the value of K is determined for CEP = 4 cm (C = 0.045 L/min) where the pressure P_e is near the maximum for the experimental GC flow rates. P_e was determined by using the average values of K_{MS} and k_{SV} (k = 0.046) in Eq. (25) rather than k_{MS} as in Fig. 14(c). This value of k is equal to k_s, the weighted average at 4 CEP. In any case, the simple average gives a curve nearly identical to that for the weighted average in the critical high pressure region of the pressure versus CEP curve. The

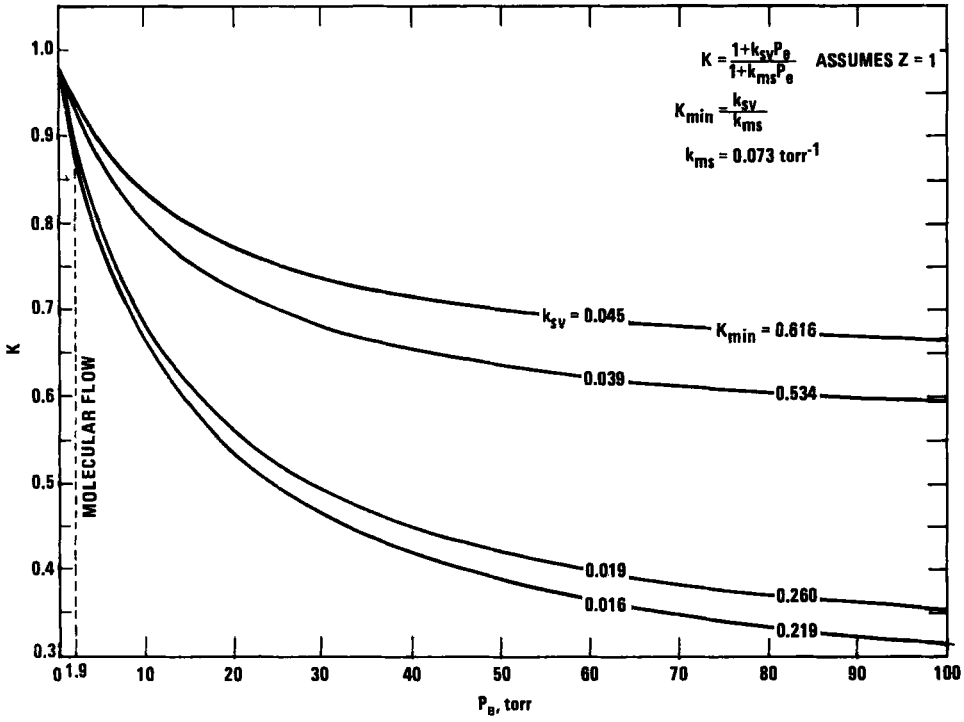

FIG. 15. Pressure factor (K) vs the GC column exit pressure (P_e) for two optional SV capillaries from each interface (see Figs. 12 and 13).

second column shows the value of K obtained assuming that both the MS and SV sections of the interface capillary were at 220°C (the same assumption was made in calculating k_{MS} and k_{SV} for the plots in Figs. 14, 15, and 16). In the third column, the values of K were determined by using the estimated average values of the MS and SV capillary temperatures. In the right-hand column, K was assumed to be unity except for the temperature correction. Although the temperature difference does tend to increase the value of K or reduce the expected pressure imbalance, the effect is not significant compared to the experimental data. In any case, temperature is not a factor in determining the effect of flow rate and pressure on the experimental CPT vs CEP curves as shown in Figs. 5 and 6 since the interface temperature distribution, however nonuniform, is the same for all the curves.

A very good approximation of the complete theoretical CPT versus CEP curve for a given GC flow rate can be obtained by using the minimum values of K from Table 1 in the set of curves shown in Fig. 16. The reason

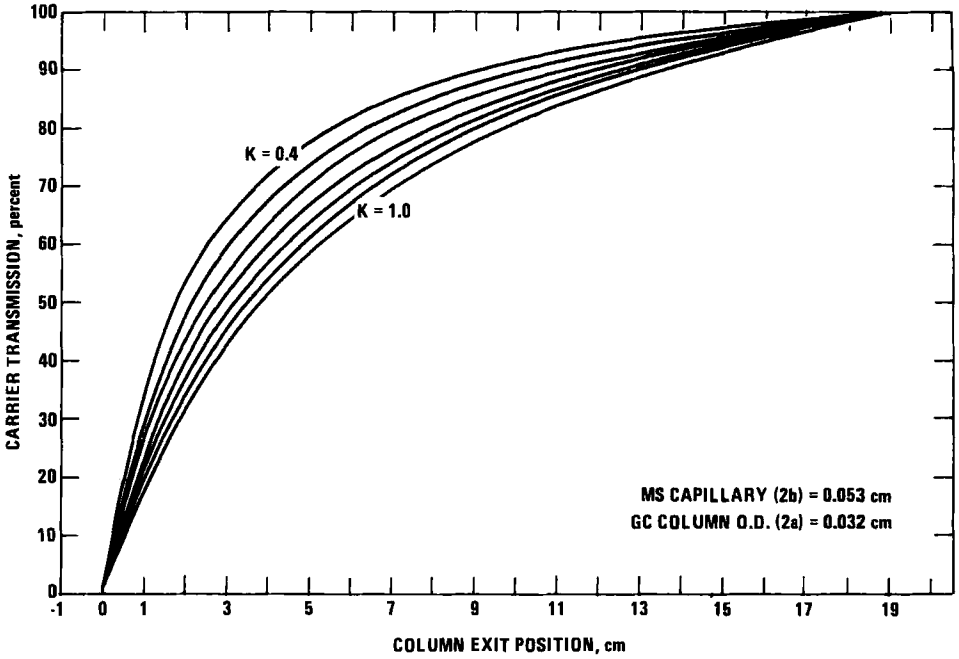

FIG. 16. The effect of the pressure factor (K) on the theoretical molecular flow CPT vs CEP curve for the experimental interface. A constant pressure is assumed for each separate curve. However, these curves are the same as the true curves for a given flow rate in the vicinity of CEP = 4 which is near the maximum interface pressure as shown in Fig. 14.

for this is that the pressure factor K does not vary significantly in the midrange of the CEP values. This can be readily verified by calculating the value of K at point-by-point pressures as discussed above and plotting the complete curve for a given flow rate. From this it becomes apparent that a percent transmission curve which takes into account the effects of interface pressure on the basis of the Knudsen relationships will be significantly different from the experimental curve.

TABLE 1

Q (sccm)	K (220°C)	K (175°C/75°C)	K = 1 (175°C/75°C)
0.64	0.73	0.74	1.12
1.1	0.65	0.67	1.13
1.6	0.60	0.63	1.15
2.7	0.54	0.57	1.18

[Successive experimental percent transmission curves using higher flow rates would be very useful since K equals K_{min} under viscous flow conditions. The same is true for curves generated with GC columns with successively larger outer diameters (the same inner diameters) since again, at some point, measurable values of K must appear as $(b - a)$ approaches zero.]

The theoretical value of K could be confirmed directly by using the Knudsen splitter (Fig. 11) at a fixed CEP corresponding to the point of maximum pressure (P_e). Constructing a complete CPT versus CEP curve by using the Knudsen splitter and a set of interchangeable circular or annular capillaries, as shown in Fig. 11, would be possible though not very convenient.

Temperature Effects

Since the temperature of the experimental interface installed in the Hewlett-Packard 5992 is not the same across its entire length, as discussed in the experimental section, the effects of temperature on flow in the transition region must be determined. An adjusted pressure factor K, which takes into account a uniform temperature gradient across the interface, can be determined. The mass flow rate through circular tubes in the molecular flow region is proportional to the absolute temperature raised to the 0.5 power, and to the -0.65 power (for helium) in the viscous flow region (*5*, *6*). In the transition flow region the effects of temperature will vary between these two extremes, depending on the exact nature of the flow as shown by Eq. (16) where k is proportional to the temperature to the 1.15 power for helium. If k_{MS} and k_{SV} (Figs. 12 or 13) are determined using the average temperature across the separate MS and SV sections of the MS transfer capillary, an accurate value of the pressure factor K can be determined as indicated in Table 1.

In Fig. 17 the mass flow rate Q through an approximately 11 cm section of the MS transfer capillary is plotted as a function of the interface pressure P_e at three different temperatures to illustrate the theoretical effect of temperature on the nature of the gas flow. Each of these curves has an inflection point (change of concavity) dependent on the Knudsen number (and temperature) at some transition pressure. Although this inflection point is not apparent in a single curve, it becomes discernable in a set of curves for different temperatures as shown even though it shifts slightly with each separate curve.

A careful comparison of a very accurate set of these isothermal Q versus P curves in the vicinity of the inflection point could serve as a means of accurately locating a transition point which is useful from a theoretical standpoint since it involves a fundamental change in the way molecules

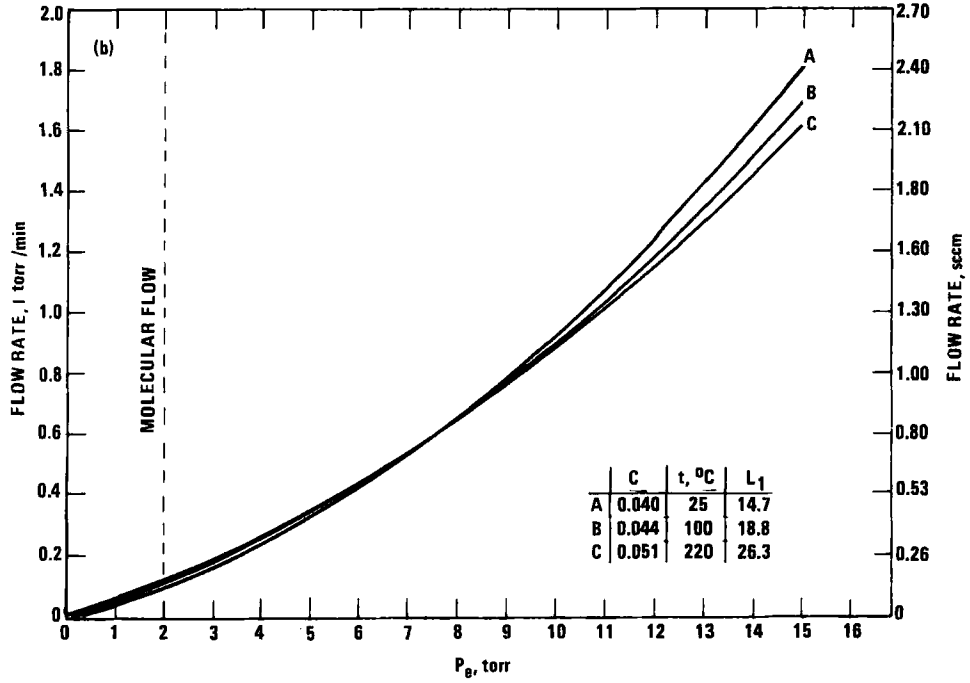

FIG. 17. Mass flow rate (Q) vs the column exit pressure (P_e) for the experimental interface at three different temperatures assuming $k_{MS} = k_{SV} = 0.073$ torr^{-1}. This same curve for 4 cm CEP also represents an equivalent 11 cm length of the MS transfer capillary.

move through the column. Another way of approximately locating a transition point which involves a fundamental property is to plot Q versus P on a log/log scale over a wide range (*3*). This transition point is revealed by the intersection of two extended straight lines, one of slope equal to unity, and the other of slope equal to 2. This curve demonstrates the 100-fold pressure range of the transition region given by Eq. (6). These same upper and lower limits to the transition region are given by $F/C = Z \approx 1$ and $F/C = kP_e$ in the extended plots of Figs. 12 and 13. The transition point is the midpoint on this log/log scale. It will be useful to determine why these two transition points (pressure and temperature) do not coincide.

Gas Flow in the GC Column

There is another important difference between the experimental interface and other atmospheric exhaust or restricted flow interfaces such as the open split interface or the supersonic jet separator. For vacuum exhaust GC, a simplified form of the Poiseuille equation for viscous gas flow

through a circular column applies so that both the mass flow rate and the flow velocity through the GC column are independent of the column exit pressure as shown by the following equations (*5*, *7*, *8*):

$$Q = 1/16(\pi a^4/L\eta)(P_i^2 - P_o^2), \qquad \text{Poiseuille equation} \tag{27}$$

The average velocity across the cross-sectional area at the column exit is obtained by applying the continuity law for flow at any point along the column so that $u_o = Q/\pi_a^2 P_o$. This, along with the Martin James factor (*7*, *20*) $J = \bar{u}/u_o = 3/2(P^2 - 1)/(P^3 - 1)$, gives the following equation for the average velocity along the column:

$$\bar{u} = 3/32(a^2/L\eta)(P_i - P_o)(P + 1)^2/(P^2 + P + 1) \tag{28}$$

where $P = P_i/P_o$.

When P becomes very large, as for vacuum exhaust GC, a simplified equation for the mass flow rate is obtained from EQ. (27):

$$Q = 1/16(\pi a^4/L\eta)P_i^2 \tag{29}$$

and since $(P + 1)^2/P^2 + P + 1$ is equal to 1 for large P, Eq. (28) reduces to

$$\bar{u} = 3/32(a^2/L\eta)P_i \tag{30}$$

Direct Measurement of the GC Flow Rate

The pumping speed of an exhaust system is given by the following equation (*9*):

$$Q = PS_{\text{eff}} = PS_p - Q_b \tag{31}$$

where Q is the net rate of carrier gas removal, P is the pressure at the inlet, and Q_b in the case of a mechanical pump is the rate at which residual carrier gas is returned to the system by the pump. S_{eff} is the effective speed of the pump, and S_p is the mechanical speed of the pump determined by the product of the frequency of rotation and the volume swept out by each revolution. Q_b is given by $Q_b = S_p P_b$, where P_b is the base pressure of a blanked-off pump. At pressures well above the base pressure, the effective speed is equal to the mechanical speed:

$$S_{\text{eff}} = S_p(1 - P_b/P) \tag{32}$$

However, since we are not interested in measuring effective pump speed but in measuring the GC flow rate, we can use the following expression from Eq. (31), where S_p is a constant:

$$Q = S_p(P - P_b) \tag{33}$$

where P is the pressure at the pump inlet.

It can be shown that since P_b is also the base pressure of the system at the point in an impedance Z_X where the pressure is measured (assuming no significant leaks):

$$Q = S_x(P_x - P_b) \tag{34}$$

where $1/S_x = Z + 1/S_p$, P_x is the measured pressure, and $(P_x - P_b)$ is the reduced pressure.

Since the mass flow rate through the GC column is unaffected by changes in the exhaust pressures over the range encountered in these experiments, as demonstrated in the previous section, the reduced pressure may be substituted for the actual pressure. This may be readily accomplished by zeroing the capacitance manometer at the base pressure rather than at its true zero pressure, as discussed previously. This reduced pressure $(P_x - P_b)$ may then be taken without error for the P_o of Fig. 1. The GC flow rate is then given by

$$Q_{GC} = S_x P_o \tag{35}$$

where S_x is the slope of a straight line which can be extrapolated to zero carrier gas flow, as shown in Fig. 3.

Chromatographic Effects

In order to preserve GC peak shape, the residence time in the MS source and the interface combined must be shorter than the GC peak width. For the source alone, this is not usually a problem. Under molecular flow conditions the equation for natural pressure decay applies, at least to a first approximation, to the half-life of sample molecules in the MS source (*1*, *3*) as well as to the residence time of a GC peak in the MS transfer capillary:

$$t_{1/2} = (V/C) \ln 2 \tag{36}$$

where C is the conductance and V is the volume.

The one important difference is that C and V cannot be varied independently of each other by geometrical design of a capillary as they may be for the MS source. The calculated value of the time constant is less valid for a column than for a two-component flow element such as the source for similar reasons.

For positive CEP values the interface is a pure conductance flow element and the residence time can be estimated from the equation for the linear velocity through a long circular tube. The average velocity of the carrier gas is given by

$$\bar{\mu} = 2C/A(kP_e + 1) \tag{37}$$

from Eq. (16) for the mass flow rate in the transition flow regime.

Assuming that the sample partial pressure is small compared to the carrier gas pressure, we can take the sample velocity to be the same as the carrier velocity at higher pressures ($kP \gg 1$). At intermediate pressures ($kP \approx 1$) there is considerable uncertainty because the interaction between sample and gas molecules also becomes a variable, and the equation for velocity contains the term $(kP + 1)^2$. At lower pressures ($kP < 1$) the conductance for the sample molecules must be used for C.

(In general, the most reliable method of determining residence time is by direct measurement, which is very difficult in this case.)

From this, it is apparent that the residence time is a factor which must be considered for a capillary of these dimensions, at least under molecular flow conditions. As the CEP increases, this borderline condition is quickly relieved because of the change from molecular to transition flow conditions. However, this is a critical factor for this interface with its long (19 cm) MS transfer capillary. The advantages of operating at low, near zero, CEP positions must be balanced against peak broadening effects. The nature of the transfer capillary surface is also important. With a chromatographic surface the actual residence time becomes less important if it is assumed that chromatographic effects are still efficient under transition carrier gas flow conditions. Under pure molecular flow conditions it is assumed that there is no chromatographic effect in the interface capillary.

Ideally, the MS transfer capillary serves as an uninterrupted extension of the GC capillary column. Since transition flow conditions are also induced in the end of the GC capillary under vacuum exhaust conditions to a distance from the end depending on its diameter and the mass flow rate, the interface may be thought of as an extended end section of the GC column. In any case, the sample is only exposed to a chromatographic surface in the interface, and GC peaks should retain their symmetrical shape even if the interface may have a peak broadening effect on higher

molecular weight compounds if it has a low isothermal temperature relative to the analytical column. Distorted GC peaks are associated with condensation effects on bare metal or glass surfaces at low temperatures, even neglecting cases of active-surface interaction with polar compounds.

Gas Flow in the End of the GC Column

It is important what effect the occurrence of nonviscous flow conditions in the end of the GC column under vacuum exhaust conditions has on the overall gas flow parameters and on GC efficiency. Sellier and Guiochon (*18*) showed from basic principles of viscous flow that when the inlet pressure is approximately atmospheric, nonviscous flow generally occurs in only a small portion of the GC column. The diameter of the column was not considered. However, because of our interest here in the properties of transition flow and the continued interest in subatmospheric inlet GC, it is worthwhile to determine quantitatively a critical inlet pressure directly in terms of the properties of the transition flow occurring at the column exit. This serves to emphasize the fact that the nature of the flow changes progressively from the end of the column back toward the inlet and that all three flow regimes will very likely exist in a column inserted directly into the E1-MS source even though the mass flow rate and average flow velocity obey the viscous flow relationships of Eqs. (29) and (30). The minimum inlet pressure for which viscous flow conditions will prevail can determined from Eqs. (6) through (9) to give $P_t = 2L_1/0.01a$, where L_1 is the mean free path at the reference pressure P_1 (1 μ), and a is the column radius. It is readily determined on this basis that overall viscous flow conditions are assured with helium as a carrier gas at atmospheric inlet pressures for all columns (at 100°C) with diameters greater than 100 μ. Another useful observation is that microbore capillaries (50 μ i.d.) would be very useful for investigating the characteristics of transition flow since injector pressures of up to 2 atm could be used.

It will also be useful to define another parameter (l_t) which is the length of the column in which transition flow occurs. In order to determine l_t, it is necessary to assume that the constant mass flow rate is determined by Eq. (29). This is a good assumption since it only breaks down as l_t approaches L, the column length. The value of l_t can then be calculated by using the corresponding value of P_t and the equation for the molecular flow conductance C. This definition of l_t is used in Fig. 18 which shows a proposed qualitative model of gas flow in the end of the GC column and in the interface. The values of l_t are equal to approximately 600 and 300 cm, respectively, for columns of 0.032 and 0.025 cm i.d. (Q = 1 sccm at 25°C.) Pure molecular flow conditions occur in the end of the column for a fraction of a centimeter in each case.

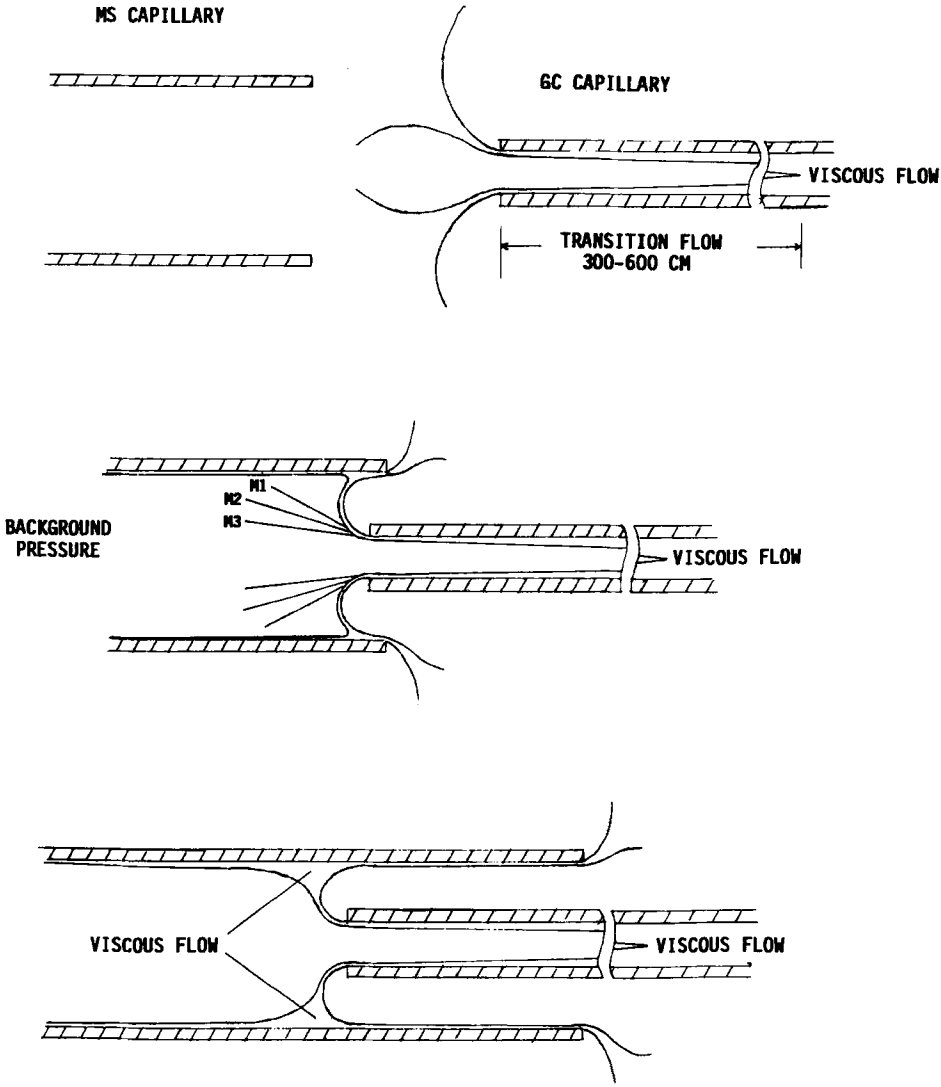

FIG. 18. Proposed gas flow pattern model for the experimental interface. The individual mass trajectories shown serve to emphasize the momentum molecualr enrichment effect. A more likely result is simply the creation of enriched solute layers within the laminar viscous stream.

The variation of GC efficiency with flow velocity as given by the Golay equation (*7*, *10*) should be another important indicator of the nature of the flow since the degree of interaction between sample molecules and carrier gas molecules becomes a variable in the transition flow region. This effect will be examined more closely in future experiments. By using these criteria, the data of previous investigators of vacuum exhaust GC/MS may be examined for indications of nonviscous flow.

In early experiments, Sellier and Guiochon (*18*) obtained accurate MS pressures using an ionization gauge over a range of GC inlet pressures from 1.1 to 2 atm in 0.1 atm intervals and calculated flow rates from 0.149 to 0.493 sccm. The experimental exhaust pressures were a precise linear function of the square of the inlet pressure over the entire range. The column (110 m × 0.25 mm i.d.) was operated at 75°C. Under these conditions the calculated value of P_i is 0.18 atm, so the flow is clearly viscous over the entire range. Only partial Golay plots of atmospheric and vacuum exhaust operation of the column were reported. In more recent vacuum exhaust GC and GC/MS experiments by Hatch and Parrish (*19*), Cramers, Scherpenzeel, and Leclerq (*7*), and Trehy, Yost, and Dorsey (*11*), the GC flow is clearly viscous according to the above criteria.

Molecular Enrichment Effects

The performance of a GC/MS interface may be conveniently characterized by the following definitions.

(1) The percent transmission of sample through the interface (SPT) or the percent yield.
(2) The percent transmission of the carrier gas (CPT) or the flow split.
(3) The ratio of (1) to (2), which is the enrichment factor E = SPT/CPT.

These definitions are similar to those described by McFadden (*1*) which were applied to traditional high flow packed column interfaces such as the Bieman Watson separator and assumed pure viscous flow to the MS and pure molecular flow to the separator vacuum. The definitions above, in contrast, permit the evaluation of the interface directly in terms of the effects of the transition flow which predominates in capillary GC/MS analysis.

For molcular flow conditions, SPT and CPT are equal and are given by the CPT verus CEP calibration curves (Fig. 2), and there should be no sample enrichment. For viscous flow conditions the flow of the trace amounts of sample is governed by the properties of the carrier gas, and the sample and carrier percent transmission is the same. However, due to

differences in molecular velocities, sample enrichment effects up to a value of $(M_s/M_c)^{1/2}$ should occur at any point in the carrier gas stream when the upstream flow is viscous and the downstream flow is nonviscous in nature. This applies to the pressure measuring electron impact MS source in particular, where the input GC flow is more or less viscous and the exhaust flow is always molecular. The sample or carrier gas partial pressure in the source is given by $P = Q/C$, where C is the molecular flow conductance of the source for sample or carrier gas molecules. This applies to discrete sample bands or peaks in a carrier gas stream as well as to a continuous flow trace gas mixture. Since molecular flow conditions exist in the MS source for all these experiments, the relative detector response will be unaffected by changes in the nature of the flow at intermediate points in an undiverted carrier gas stream. (This requirement for molecular flow conditions in the MS source apparently more or less coincides with the requirement for no intermolecular collisions necesary to insure reproducible ion fragment levels.)

However, measurable sample enrichment effects should occur at the split point in the interface over a pressure range where the gas flow is more molecular in nature in the SV capillary than in the MS capillary. The maximum value of this velocity enrichment should occur at that pressure P_e (and CEP) where the difference is the greatest. This difference is related to the pressure factor K, since E_v equals 1 when K equals 1 (molecular flow in both capillaries) and also when $K = K_{\min}$ (viscous flow in both capillaries). On this basis, at least it is logical to assume that $E_v(\max)$ occurs at a pressure corresponding to an inflection point in the K vs P_c curve between two extremes (Fig. 15). The more accurate form of the curve, in which the assumption that Z is equal to 1 is not made, would be required to accurately locate such an inflection point.

An approximate theoretical enrichment factor can be determined on this basis since it can be shown by using Eqs. (6)–(19) that the sample percent transmission (SPT) is given by a relationship identical to that for carrier percent transmission (CPT) except that k_{MS} and k_{SV} in the expression for the pressure factor K (Eq. 19) are replaced by k'_{MS} and k'_{SV} where $k' = k(M_s/M_c)^{1/2}$ in both cases. Then the assumption is made that $Z = 1$ and that $(F_v)_s = (F_v)_c$ and $C_s = C_c(M_s/M_c)^{1/2}$. The velocity enrichment factor is then simply SPT/CPT, where both SPT and CPT are given by Eq. (18) except that the pressure factor K is replaced by K' for SPT. Under molecular flow conditions, both K and K' are equal to unity. A more accurate enrichment factor would require the use of the binary mean free path and the mole fraction as well as consideration of diffusion effects and the parabolic velocity profile across the tube cross section in determining k' and K'.

Performance curves are developed in Fig. 19 by using the pressure factor K for an interface with the most efficient cross-section dimensions (smallest annular space: $b - a$). These curves demonstrate two important points. First, this experimental interface is not a particularly efficient type of effusive separator since the maximum value $M_s/M_c)^{1/2}$ can never be approached because of the interdependence of the performance criteria. This problem was avoided to a large extent in effusive separators, such as the Bieman-Watson separator for packed columns, because the sintered glass is made up of an extremely large number of long narrow bore capillaries which permit high separator vacuum flow even under pure molecular flow conditions. The second point is that no velocity enrichment at all should occur in the CEP range (-6 to 0) where the maximum molecular enrichment is observed experimentally (Figs. 7 and 9) since molecular flow conditions exist in the interface capillaries as shown by the pressure versus CEP curves of Fig. 14 as well as in the end of the GC capillary itself. It should be noted, however, that even a small enrichment factor of 1.5 or less can serve a very useful function, particularly for an interface of this type which serves as an extension of the GC column. Frequently only a small split by one-half or less of the optimum GC flow rate is required to produce an acceptably low MS source pressure. Thus maximum GC peak resolution can frequently be achieved with only a small reduction in MS sensitivity. For the analysis of complex trace mixtures this is a very desirable tradeoff. Even then a small loss in yield may be counter balanced by the narrower more intense peaks.

The sharp peak in E_v observed for a constant GC flow rate (Fig. 19c) is a result of the two competing factors involved as the CEP is reduced to zero. First, as illustrated in Fig. 19(b), E_v tends to a maximum at constant pressure as the CEP is reduced, and second, E_v approaches zero as the pressure approaches zero at a fixed CEP as shown in Fig. 19(a). The exact shape of this peak observed experimentally should be strongly influenced by the exact value of Z which has been assumed to be 1 for these graphs and the peak should not be so pronounced for the larger values of $(b - a)$ used experimentally.

The close agreement, as shown in Figs. 5 and 6, of the experimental percent transmission curves with the theoretical molecular flow curve is not predicted by the Knudsen relationships, as discussed earlier. Molecular flow conditions for the experimental interface exist only at very low and very high CEP values for these GC flow rates (Fig. 14b). At all intermediate CEP values the flow is in the transition region and the pressure factor K is less than unity (Fig. 15). It is, however, important that molecular flow conditions exist in the external SV exhaust system when the GC column is in negative CEP positions in order for the assumption to hold that the

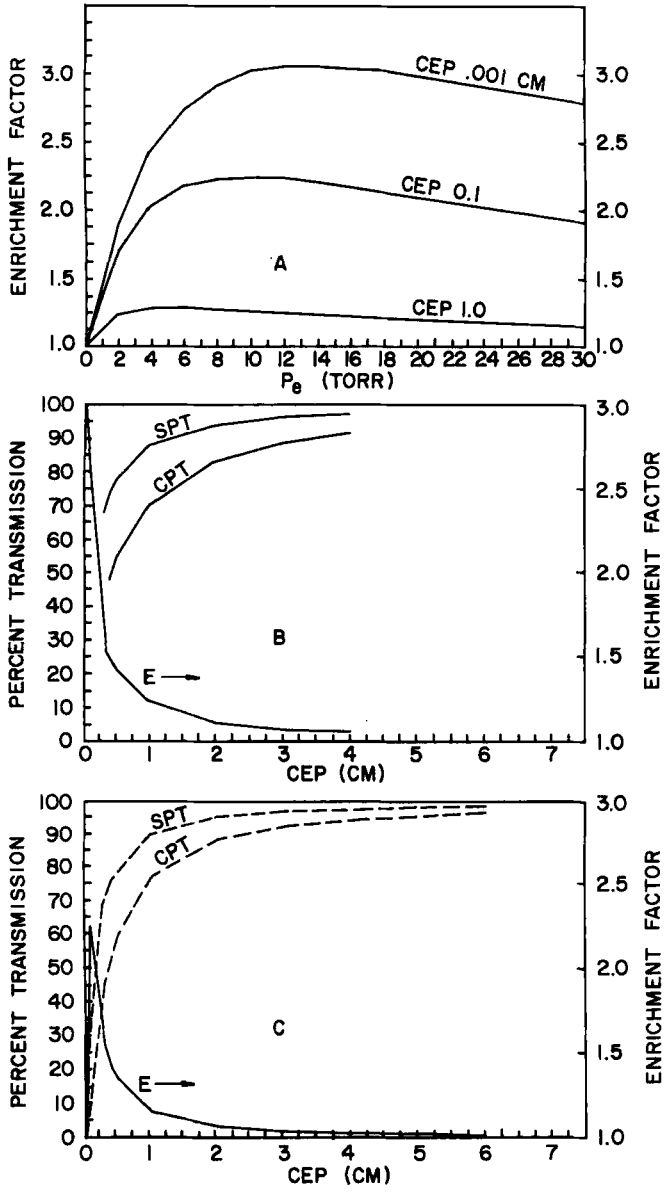

FIG. 19. Some theoretical values of the performance criteria for the experimental interface. (A) Enrichment factor (E_V) vs pressure (P_e) at a fixed CEP. (B) Enrichment factor vs CEP at a fixed pressure (P_e = 14 torr). (C) Enrichment factor vs CEP at a constant GC flow rate (Q_{GC} = 3 sccm). E_V = SPT/CPT, A = 0.849, $(M_s/M_c)^{1/2}$ = 10, k_{MS} = 0.073, k_{SV} = 0.007.

enrichment factor approaches unity as the GC column is withdrawn. If the GC flow is more molecular in the MS capillary than in the external SV system, inverse enrichment will occur and a true reference value cannot be obtained. (R_1 in Eq. 4 will not be equal to the sample-to-carrier ratio of the GC effluent). This could result in the measurement of incorrect high experimental enrichment values at positive CEP positions and could possibly account for the greater than 100% experimental yield observed ($Y = E \times \text{CPT}$). It might seem that this could be the case even for the low experimental pressures (10–200 μ) since the i.d. of the critical flow element in the external SV system (0.6 cm) is much greater than the i.d. of the MS transfer capillary (0.053 cm), and in this case k_{SV} is much greater than k_{MS}. This is just the opposite of what occurs for positive CEP values, as shown in Fig. 13.

However, it can be seen from Eqs. (34) and (35) that the impedance of the connecting tubing ($Z = 0.008$ min/L) is small compared to the pump impedance ($1/s_p = 0.043$) and the conductance S_x is nearly equal to the pump speed (Appendix 6). Thus the nature of the flow through the connecting tubing has only a small effect on the overall flow properties of the external exhaust system. The linear relationship up to 180 μ shown in Fig. 3 is evidence of this. The validity of the reference value R_1 over the entire experimental pressure range is thus assured in this respect.

The Measured Rotary Pump Speed

The reason for the low apparent speed of the rotary pump (23.2 L/min) compared to the value quoted by the manufacturer (60 L/min for helium) must be explained.

It has been suggested that a rotary pump should have an effect similar to that of a critical orifice as a flow element (*9*). On this basis the pump speed should be constant and independent of pressure in the molecular flow range and also independent of pressure in the viscous flow range since the pressure ratio ($r = P_b/P$) is always less than a critical value at these higher flow rates.

The pump speed verus pressure curve of Fig. 20 has been constructed by combining the experimental data of Fig. 3 for the molecular flow region with the high pressure section of the pump speed versus pressure curve furnished by the manufacturer. The intermediate transition flow region of the curve was created by a reasonable extension of the nonlinear portions of the other sections. The pump speed in the molecular flow region of the manufacturer's curve is pressure dependent because the effective speed is being plotted rather than the mechanical speed as discussed in the devel-

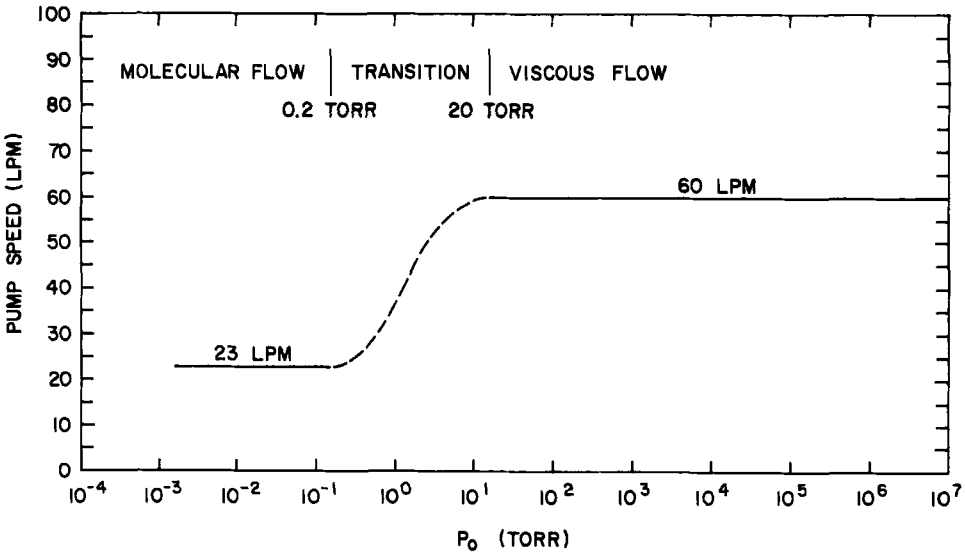

FIG. 20. Suggested performance curve for E2M2 rotary pump.

opment of Eqs. (34) and (35). It is apparent that a curve such as Fig. 20 would be much more useful than the manufacturer's curve in characterizing the performance of a GC/MS interface pump.

In the molecular flow region the pump speed (S_p) can be directly related to the frequency of rotation and the sweep volume of the pump. This is important since it means that an accurate and reproducible calculation of system conductance can be made even when the pump is the principal flow element. In this case a very high speed pump would be required to remove pump speed as a factor in the calculation of system pumping speed.

For this reason a more thorough investigation of this means of determining rotary pump speed should be undertaken. An accurate curve, such as shown in Fig. 20, could be generated experimentally over the entire pressure range since the exhaust pressure P_o will always be much lower than GC column inlet pressure P_i, and the simplified form of the Poiseuille equation will always apply when the column is in the withdrawn or negative CEP position.

A Comparison between the Experimental Separator and the Knudsen Splitter

The experimental separator could be readily converted to a Knudsen splitter, as shown in Fig. 11, by the insertion of a long wide bore (1.25

cm) flow element in the SV system which is fitted on the inside with a standard $^1/_{16}$ in. swagelock fitting for holding fused silica capillaries of various lengths. This wide bore flow element may also be fitted with a sidearm on the pump side of the fused silica capillary for measuring P_o, while another high pressure gauge (BHA 200-10K) is used for measuring P_e. The GC capillary should be at its most negative position.

Although a Knudsen splitter has little practical utility as a GC/MS interface, it is very important here from a theoretical standpoint. Not only can it be used to directly confirm the Knudsen molecular flow equations, it can be used to measure directly the flow characteristics of the experimental interface which, according to conventional theory, should be the same for both devices under equivalent conditions and which cannot be measured directly with the experimental interface. A comparison between the two devices is summarized in Table 2.

Experiments involving a variable CEP are readily performed by using the experimental interface, while experiments involving variable pressure at a fixed CEP are readily performed by using the Knudsen splitter. Although it would be very time consuming to generate entire CEP curves, very important experiments using the Knudsen splitter could be carried out at critical CEP values for direct comparison to the data at the corresponding experimental interface CEP as shown in Table 2.

A suggested explanation for the predicted differences is that the Knudsen splitter has essentially the same configuration that has been used to verify the Knudsen equation in the past to the extent that both the MS and SV capillaries in the Knudsen splitter are isolated from external flow effects at each end. In the experimental interface in contrast, flow through the interface capillaries is essentially continuous with the GC capillary flow so that the gradual transition from viscous to molecular flow is never completely disrupted.

In the Knudsen splitter (Fig. 11) the interface volume is assumed to be sufficiently great so that any flow affects between the capillaries are negligible.

Molecular Beam Effects

Adamczyk and Michalak (*14*) have presented a practical model for the effusion of a molecular beam from a tube at right angles to an electron beam in an open conductance MS source. The intensity distribution of a molecular beam, simulated experimentally using a light beam, is based on the cosine law modified for a long tube ($L \gg r$) (*3*, *17*). The dependence of the intensity distribution on the length of the tube, the distance of the electron beam or detector from the end of the tube, and the alignment of the electron beam with the end of the tube is demonstrated. This model

TABLE 2
A Comparison between the Experimental Separator and the Knudsen Splitter

Knudsen splitter (Fig. 11)	P_e vs CEP	F/C vs P_e	CPT vs CEP	K vs P_e	K vs T	E vs CEP
Theoretical curves	Same as for Experimental Separator provided $l_{MS} + l_{SV} = L$	Fig. 12 (Eq. 22) for individual MS and SV capillaries $F/C = kP_e + 1$ For splitter as a unit, $k = k_s$ (defined in previous column)	Fig. 2 (Eq. 1) for molecular flow conditions Fig. 16 (Eq. 18) for transition flow conditions	Fig. 15 (Eq. 19) upper set of curves $K = 1$ (molecular flow) $K = \frac{K_{SV}P_e + 1}{K_{MS}P_e + 1}$ (trans) $K = \frac{k_{SV}}{K_{MS}}$ (viscous)	$K = \frac{1 + k^*_{SV}T^{1.15}}{1 + k^*_{MS}T^{1.15}}$ where k^* is the constant pressure equivalent of the constant in Eq. (19)	Fig. 18(a–c) for velocity enrichment No momentum enrichment (E_m) is possible
Experimental curves	Accurate values of P_e possible over entire range of Q_{GC} flow rates at selected l_{SV}/l_{MS} ratios	Accurate values of $(F/C)_s$ can be obtained at selected l_{SV}/l_{MS} ratios using experimental values of P_e and flow Q	Accurate values of CPT can be obtained at selected l_{SV}/l_{MS} ratios provided $l_{MS} + l_{SV} = L$	K can be determined accurately over entire flow range at selected l_{SV}/l_{MS} ratios using experimental values of P_e	K could be determined accurately as a function of either the interface temperature or of the separate capillary temperatures	Possible by direct measurement of E_v at selected l_{SV}/l_{MS} ratios

Experimental separator (Fig. 1)	P_e vs CEP	FC vs P_e	CPT vs CEP	K vs P_e	K vs T	E vs CEP
Theoretical curves	Fig. 14(a) (Eq. 24). Molecular flow conditions Figs 14(b) and 14(c) (Eq. 25). $k = k_{MS}$ for this curve. For accurate point by point, curve k_s equals $\frac{k_{MS}C_{SV} + k_{SV}C_{SV}}{C_{MS} + C_{SV}}$	Fig. 13 (Eq. 22) for individual SM and SV capillaries $k_c = \frac{0.147}{3L_1}(b - a)$ (annular) $k_c = \frac{0.147}{2L_1}(b)$ (circular) $k_s \approx \frac{k_{MS} + k_{SV}}{2}$	Fig. 2 (Eq. 2) for molecular flow	Fig. 15 (Eq. 19) lower set of curves (different k_{SV}) Fig. 16, K vs pressure as a function of CEP	K should change as a function of interface temperature only under transition flow conditions	Fig. 18(a–c) for velocity enrichment E_v Apparently no theoretical equation has been developed for momentum enrichment (E_m) under these low pressure conditions
Experimental curves	None possible	None possible	Figs. 5 and 6. Same curve obtained for both molecular flow and transition flow conditions	Figs. 5 and 6. No displacement of CPT vs CEP curve from molecular flow curve. Therefore $K = 1$ over range of experimental pressures and flow rates	The displacement of CPT vs CEP curve could be used to determine K as a function of interface temperature	Figs. 7–9 for momentum enrichment (E_m) Since $K = 1$ (Fig. 5), there should be no E_v since E_v is dependent on K

could apply to the flow from the GC capillary into the interface cavity at negative CEP values as well as flow from the MS transfer capillary or directly inserted GC capillary into the MS source since the Knudsen number in the end of the GC capillary varies between approximately 4 (Fig. 7a) and 1 (Fig. 7b) for the molecular enrichment experiments. This model presents a sharp contrast to the proposed gas flow model of Fig. 18 in many ways. For example, there is no centerline molecular enrichment in a molecular beam as shown by the cosine law. Again a distinction is suggested between the nature of flow in a capillary of a given length and flow in the same length at the end of a very long capillary. From the Adamczyk model it can be seen that the experimental GC/MS interface configuration, as shown in Fig. 1 with its long circular MS transfer capillary, is not a very effective system for producing an intense molecular beam for GC/MS analysis. The percent transmission is very low (<1%) for negative CEP values, and the interface manifold pressure P_o must be reduced to levels much less than are used here to achieve a long mean free path in order to avoid further severe attenuation of the molecular beam intensity. While a general rule is that for maximum molecular beam flux density the source gas mean free path should be less than the length of the tube and greater than its radius, this must be altered somewhat for CEP values near zero because of the directional character of the GC effluent molecular velocities. With a very short source attached MS transfer capillary (*13*), the probability would increase for an intense molecular beam in the MS source as the CEP approaches zero from negative CEP values.

It is apparent that with an open MS source and a moveable, narrow magnetically collimated electron beam, the flow pattern of the GC effluent emerging from the MS transfer capillary could be carefully mapped out and any molecular enrichment occurring in the source itself could be detected using SIM analysis, as demonstrated previously. It is important to note in this regard that the flow pattern at the interface and in the MS source are separate though related problems and that the first has a direct bearing on the second. Any experimental observations regarding the nature of this flow at the MS end can be used to predict a flow model for the interface cavity.

CONCLUSION

It seems apparent that the experimental interface can serve a useful purpose for many GC/MS systems, and equally apparent that many more useful applications could develop as the transmission characteristics of the interface become thoroughly documented and explained.

Three significant features of the experimental data stand out:

(1) The carrier gas percent transmission is independent of interface pressure in the nonmolecular flow region, which implies that the nature of the flow is always identical in the MS and SV capillaries, despite apparent theoretical differences.
(2) Much higher sample enrichment effects are observed than can be accounted for under these low exhaust pressure conditions.
(3) The MS detector response is clearly nonlinear with respect to both carrier gas and sample pressure as the CEP is changed.

These results appear to be related, and they suggest the need for further research in an area where there appears to be little analytical data available from the literature. It seems apparent from the experimental data presented here that there may be a significant difference between the transition flow which occurs both in the interface capillaries and in the end of the GC capillary as a result of the gradual decrease in pressure along the column from the viscous flow of the column proper, and that transition flow defined by the Knudsen relationships which occurs in a separate capillary isolated from such a flow stream.

The transmission characteristics of the interface can be clearly defined by the analytical methods described here, carried out on a more extensive and accurate scale. The differences between the experimental interface and the Knudsen splitter may also be clearly defined in the manner summarized in Table 2. The Knudsen splitter as described here also appears to offer some advantages over previous devices in examining the Knudsen molecular flow equations on a more accurate basis.

It is suggested that the existence of an annular viscous carrier gas stream under overall transition flow conditions in the GC and interface capillaries would be very useful in accounting for these anomalous experimental results. If the stationary boundary gas layer that characterizes viscous flow in columns remains stationary in the transition region as well, the existence of a distinct gradually collapsing annular flow stream could be postulated in a logical extension of the kinetic theory of viscosity as a result of the gradual appearance of molecular flow conditions at the center of the GC column as the overall pressure decreases to the molecular flow level toward the end of the column. Such a mechanism offers a plausible alternative to the Knudsen transition flow equations and to the concept of slip at the column surface to account for the apparent change in the nature of flow in the transition region although slip flow is, strictly speaking, only defined in the high pressure end of the transition region.

The role of the liquid polymer surface of the interface capillaries may be very important in this respect for both molecular and transition flow since the liquid film could be considered a near perfect surface for molecular collisions with the column wall. It would be expected that except for very small angles of incidence, these collisions would result in adsorption and subsequent evaporation at a random angle, thus reducing the fraction of specular reflections to near zero. The relative fraction of diffuse and specular reflections should also affect the molecular flow equations since they all assume the fraction (f) of diffusive (random) reflections to be unity. The effect of different column surfaces on molecular and transition flow has been examined by Brown et al. (*15*).

A hypothetical flow model based on this approach, which may very well satisfy the requirements of the experimental data, is shown in Fig. 18. Obviously, any attempt to rigorously de-find the existence of such a radical flow pattern is beyond the scope of this paper and of the author's work at the present time. However, some qualitative observations can be made in view of the analytical data.

Although it is certain that at least statistically, either at equilibrium or at some prior time, there will be two opposite flowing concentric (central and annular) gas streams extending some finite distance into the transfer capillary. The creation at any time of a free floating but well-defined boundary layer between them, however advantageous to the hypothetical model, is apparently not required. In order for the flow stream to reverse itself, the existence of any nonmolecular flow is also not required since the direction and rate of molecular flow is explained by theory purely on a statistical basis. However, if we pursue an argument similar to that used for the flow pattern in the end of the GC column, the creation of a self-constrained gas flow stream at the point of flow reversal, as shown in the diagram, logically follows even without the prior existence of annular GC column flow. In the first case, the creation of a viscous flow component not parallel to the axis of the GC column is caused by gradual uncoupling of carrier gas molecules at the center of the flow stream. In the second case, coupling occurs at the stationary boundary layer between the opposite flowing streams and centrifugal acceleration creates a constraining viscous force at right angles to the direction of flow which opposes the centrifugal force and causes the gas stream to occupy a minimum space and follow a circular path. Molecular enrichment may then result from momentum separation in the centrifugal force field. In any case, whatever the exact enrichment mechanism proves to be, its experimental measurement, and GC/MS analysis in general, offers a new approach to an old problem.

A follow-up paper is planned which will attempt to differentiate between the gas flow pattern of the experimental separator and that of other mo-

mentum separators, such as the opposed jet isotope separator, which the author had not considered when this paper was first submitted.

APPENDIX 1

Flow element	a (cm)	L (cm)	C (L/min)	$1/C$ (min/L)
1	0.6	2 × 8	215	0.0046
2	0.8	2 × 8	505	0.0020
3	1.25	10 + 7	1815	0.00055
4	0.9	9	1300	0.00077
				Z = 0.00792 mpL or 126 L/min

APPENDIX 2

amu	EM V	ms
71	2600	500
4	1000	300

APPENDIX 3

An accurate value for the viscosity of helium in the range of GC temperatures can be obtained by using the relation $\eta = aT^n$ where $a = 4.61 \times 10^{-6}$ and $n = 0.659$. These constants were obtained from a log/log plot of the values of the viscosity at selected temperatures over this range which are listed in the *CRC Handbook*, where $a = n_0/T_0$ and n is the slope of the straight line. Although these values of η are not used in each instance in this paper, the differences are never significant.

APPENDIX 4

It is unfortunate that $(b - a)$ was used to designate the flow space in an annular capillary in this paper since the reverse designation, $(a - b)$ as used in Lafferty and Dushman (*3*), is more convenient and avoids confusion in comparing circular and annular capillaries. The $(a - b)$ designation will be used in the future.

APPENDIX 5

a	b	$2/3(b - a)$	X	Y	Z
0.026	0.0265	0.000333333	0.000333335	0.001446256	0.001446254
0.025	0.0265	0.001000000	0.001000057	0.003280980	0.003280934
0.024	0.0265	0.001666667	0.001666939	0.004789308	0.004789112
0.023	0.0265	0.002333333	0.002334113	0.006133605	0.006133093
0.022	0.0265	0.003000000	0.003001730	0.007368593	0.007367532
0.021	0.0265	0.003666667	0.003669967	0.008521583	0.008519667
0.020	0.0265	0.004333333	0.004339037	0.009608780	0.009605621
0.019	0.0265	0.005000000	0.005009188	0.010640825	0.010635943
0.018	0.0265	0.005666667	0.005680720	0.011625197	0.011618000
0.017	0.0265	0.006333333	0.006353990	0.012567409	0.012557182
0.016	0.0265	0.007000000	0.007029433	0.013471686	0.013457562
0.015	0.0265	0.007666667	0.007707576	0.014341362	0.014322294
0.014	0.0265	0.008333333	0.008389071	0.015179142	0.015153866
0.013	0.0265	0.009000000	0.009074728	0.015987279	0.015954264
0.012	0.0265	0.009666667	0.009765566	0.016767702	0.016725086
0.011	0.0265	0.010333333	0.010462891	0.017522118	0.017467622
0.010	0.0265	0.011000000	0.011168399	0.018252103	0.018182909
0.009	0.0265	0.011666667	0.011884342	0.018959195	0.018871778
0.008	0.0265	0.012333333	0.012613786	0.019644998	0.019534880
0.007	0.0265	0.013000000	0.013361030	0.020311336	0.020172715
0.006	0.0265	0.013666667	0.014132350	0.020960487	0.020785641
0.005	0.0265	0.014333333	0.014937369	0.021595606	0.021373895
0.004	0.0265	0.015000000	0.015791914	0.022221579	0.021937596
0.003	0.0265	0.015666667	0.016724732	0.022847002	0.022476754
0.002	0.0265	0.016333333	0.017797108	0.023489924	0.022991270

$$X = [b^2 + a^2]/(b - a) - (b + a)/\ln(b/a)$$

$$Y = [b^4 - a^4 - (b^2 - a^2)^2/\ln(b/a)]^{0.25}$$

$$Z = [2/3(b^2 - a^2)(b - a)^2]^{0.25}$$

X is the characteristic dimension of an annular column taken from Eq. (21). X equals $2/3(b - a)$ for small $(b - a)$ as shown above.

Y is the radius of a circular column whose viscous flow conductance is the same as an annular column with annular space $(b - a)$. Y equals Z for small $(b - a)$ as shown above. The significant fact here, however, is that the terms inside the brackets for Y and Z are equal.

The range of values applicable to the experimental work is bounded by the underlines.

APPENDIX 6

S_x = 19.5 L/min (Fig. 3)
S_{tube} = 126 L/min (Appendix 1)
$1/S_x = 1/S_p + 1/S_{\text{tube}}$
$1/S_p = 0.051 - 0.008 = 0.043$
S_p = 23.2 L/min

Acknowledgments

Although the research described in this article has been funded in part by the United States Environmental Protection Agency through Cooperative Agreement R810008 entitled "Airborne Toxic Substances," it has not been subjected to the Agency's required peer and policy review and therefore does not necessarily reflect the reviews of the Agency, and no official endorsement should be inferred. The experimental work was carried out by the author for the University of North Carolina at the U.S. Environmental Protection Agency at Research Triangle Park, North Carolina. The author wishes to thank Donald L. Fox of the Department of Environmental Science and Engineering at the University of North Carolina at Chapel Hill for earlier editing assistance, and Hal Mann of the Physics Shop for construction of the experimental interface.

REFERENCES

1. W. H. McFadden, *Techniques of Combined Gas Chromatography/Mass Spectrometry,* Wiley-Interscience, New York, 1973.
2. C. M. Van Atta, *Vacuum Science and Engineering,* McGraw-Hill, New York, 1965.
3. J. M. Lafferty and S. Dushman, *Scientific Foundations of Vacuum Technique,* Wiley, New York, 1966.
4. W. G. Pollard and R. D. Present, *Phys. Rev., 73,* 762 (1944).
5. L. S. Ettre, "Viscosity of Gases Used as the Mobile Phase in Gas Chromatography," *Chromatographia, 18*(5) (1984).
6. W. Licht and P. G. Stechert, *Phys. Chem., 48,* 23 (1944).
7. C. A. Cramers, G. Scherpenzeel, and P. A. Leclerq, *J. Chromatogr., 203,* 207–216 (1981).
8. G. Guiochon, "The Flow of Gases in Porous Media," *Chromatogr. Rev., 8* (1966).
9. A. Guthrie and R. K. Wakerling (eds.), *Vacuum Equipment and Techniques,* McGraw-Hill, New York.
10. P. M. Schutjes, P. A. Leclerq, J. A. Rijks, C. A. Cramers, Vidal-Madjar, and G. Guiochon, *J Chromatogr.,* 289, 163–170 (1984).
11. M. Trehy, R. Yost, and J. G. Dorsey, *Anal. Chem., 58,* 14–19 (1986).
12. D. Sharp, "Variable Molecular Separator," U.S. Patent 4,654,052 (March 31, 1987).
13. D. Sharp, "Internal GC/MS Interface," U.S. Patent 4,641,541 (February 10, 1987).
14. B. Adamczyk and L. Michalak, *J. Mass. Spectrosc. Ion Processes, 69,* 163–174 (1986).
15. G. P. Brown, A. Dinardo, G. K. Cherg, and T. K. Sherwood, *J. Appl. Phys., 17,* 802 (1946).
16. E. G. Kennard, *Kinetic Theory of Gases,* McGraw-Hill, New York, 1938.

17. N. F. Ramsey, *Molecular Beams*, Clarendon Press, Oxford, 1956.
18. N. Sellier and G. Guiochon, *J. Chromatogr. Sci.*, *8*, 147–150 (March 1970).
19. F. Hatch and M. Parrish, *Anal. Chem.*, *50*, 1164–1168 (July 1978).
20. A. T. James and A. J. P. Martin, *Biochem. J.*, *50*, 679 (1952).

Received by editor March 12, 1987
Revised March 9, 1990